



HORIZON EUROPE PROGRAMME – TOPIC: HORIZON-CL5-2022-D5-01-02

AENEAS

Innovative Energy storage systems Onboard vessels

Deliverable 2.4: Verified and validated pre-design model

Primary Author(s)	Sokratis Mamarikas, Spyridon Spyridopoulos AUTH Franck Sellier SIE
Deliverable Type	Report
Dissemination Level	PU - Public
Due Date (Annex I)	31.07.2026 (Month 30)
Pages	66
Document Version	Draft 2.0 (Final)
GA Number	101095902
Project Coordinator	Mohsen Akbarzadeh Flanders Make (FM) (Mohsen.Akbarzadeh@flandersmake.be)

Contributors			
Name	Organisation		
Spyridon Spyridopoulos	AUTH		
Sokratis Mamarikas	AUTH		
Leonidas Ntziachristos	AUTH		
Grigorios Koltsakis	AUTH		
Franck Sellier	SIE		
Formal Reviewers			
Name	Organisation		
Cosimo Cervicato	GRIM		
Mohsen Akbarzadeh	FM		
Version Log			
Rev #	Date	Author	Description
0.1	30.07.2025	Sokratis Mamarikas, Spyridopoulos Spyridon, Franck Sellier	Document creation
0.2	30.11.2025	Sokratis Mamarikas, Spyridopoulos Spyridon, Franck Sellier	First draft
1.0	08.01.2026	Sokratis Mamarikas, Spyridopoulos Spyridon, Franck Sellier	Final version
1.1	14.01.2026	Cervicato Cosimo (GRIM)	Quality review
1.2	15.01.2026	Mohsen Akbarzadeh (FM)	Quality review
1.3	26.01.2026	Anesa Begovic (I2M)	Formatting check
2.0 (Final)	26.01.2026	Mohsen Akbarzadeh (FM)	Coordinator review and approval, deliverable ready for submission

Project Abstract

AENEAS aims to advance climate-neutral and environmentally friendly water transport through the development of three innovative clean energy storage solutions. These next-generation solutions, namely Semi-Solid-State Battery (SSSB), SuperCapacitor (SC), and a Hybrid system combining SSSB and SC, go beyond the traditional battery systems. Their primary goal is to enable (partial or full) electric shipping, accommodating various ship types and challenging conditions, including adverse weather and in-land waterways. Eventual impact is an increase of the global competitiveness of the EU waterborne transport sector by European technology leadership for energy storage solutions for diverse waterborne applications. AENEAS will evaluate these solutions for a range of applications in short-sea shipping and in land waterways, enhancing their global competitiveness. Simultaneously, AENEAS will define the pathway for Energy Storage Solutions (ESSs) in different ship types, ensuring a comprehensive understanding of their applicability and potential impact on diverse waterborne transport.



Table of Contents

1	Public summary.....	5
2	Introduction	6
2.1	Overall methodology	7
2.2	Ship-powertrain models	9
2.2.1	Modeling background in the platform of Simcenter Amesim	9
2.2.2	Ship models (baseline & AENEAS integrations) for Use-Case 1	15
2.2.2.1	Baseline ship model	15
2.2.2.2	Ship model after AENEAS solutions integration.....	19
2.2.3	Ship models (baseline & AENEAS integrations) for use-case 2.....	21
2.2.3.1	Baseline mode.....	21
2.2.3.2	Ship model after AENEAS solutions integration.....	25
2.2.4	Ship models (baseline & AENEAS integrations) for use-case 3.....	27
2.2.4.1	Baseline ship model	27
2.2.4.2	Ship model after AENEAS solutions integration.....	29
2.3	Operating situations	31
2.3.1	Overall parameters examined	31
2.4	Simulations with Monte Carlo.....	34
2.4.1	Monte Carlo Method overview description.....	34
2.4.1.1	MATLAB-Simcenter Amesim connection and Model Execution	34
2.4.1.2	Sampling and Required Sample-Size Selection.....	35
2.4.1.3	Statistical Consistency Check (Kolmogorov–Smirnov Test).....	36
2.4.1.4	Post-Processing and Result Analysis	37
3	Results for use-case 1.....	40
3.1	Cumulative CO ₂ Emissions Results.....	40
3.1.1	Cumulative Emissions comparison.....	40
3.1.2	Target variable distribution identification and characterization.....	42
3.1.3	Hypotheses Analysis on input variables	44
3.2	Sensitivity Analysis on Input Variables	45
3.3	Reduced surrogate models	46
4	Results for use case 2.....	49

4.1	Cumulative CO ₂ Emissions Results.....	49
4.1.1	Cumulative Emissions distribution comparison.....	49
4.1.2	Target variable distribution identification and characterization.....	51
4.1.3	Hypotheses Analysis on input variables	52
4.2	Sensitivity Analysis on Input Variables	53
4.3	Reduced surrogate models	53
5	Results for use case 3.....	56
5.1	Cumulative CO ₂ Emissions Results.....	56
5.1.1	Cumulative Emissions distribution comparison.....	56
5.1.2	Target variable distribution identification and characterization.....	57
5.1.3	Hypotheses Analysis on input variables	58
5.2	Sensitivity Analysis on Input Variables	58
5.3	Reduced surrogate models	59
6	Conclusions.....	60
7	References.....	61
8	Acknowledgements and disclaimer	62
9	Abbreviations and Definitions	63



1 Public summary

This Deliverable (D2.4) evaluates the impacts at the complete ship level of integrating the Energy Storage Systems (ESS) developed in the AENEAS project, with particular focus on the proposed sizing approach and energy management optimization strategy.

The primary objective is to verify the viability and to quantify the reduction in CO₂ emissions/fuel consumption achieved by transitioning from typical base-case hybrid and conventional vessels to optimized electrified architectures that are equipped with advanced ESS technology and new energy management strategies across three distinct maritime use cases; a RO-RO, a RO—Pax and an inland shipping vessel.

To ensure the reliability of this comparison, this Deliverable uses detailed physics-based ship powertrain models and a Monte Carlo simulation process. This stochastic approach allows the model to account for the inherent uncertainties in maritime operations, such as fluctuating weather conditions and variable cargo loads. By running hundreds of simulated scenarios, the Monte Carlo method provides a high-confidence probabilistic view of potential CO₂ savings rather than just a single optimistic estimate.

Results verify the viability of the AENEAS solutions given that they lead to fuel and CO₂ emission benefits.

2 Introduction

This Deliverable (D2.4) of AENEAS refers to Task 2.4 and involves ensuring the viability of the developed controls and strategies through simulation with a digital twin. The result is verification and validation of the preliminary design model.

The deliverable actually focuses on verifying and validating the optimized electrified architecture developed in earlier tasks across the 3 use cases defined in WP1. The goal is to verify the effectiveness and robustness of the optimized control and energy management strategies through digital twin simulations avoiding the need for physical testing. The evaluation process consists of two main stages:

1. Robustness evaluation:

The optimized pre-design models developed in Task 2.2 are re-used and assess their performance under a variety of operational and mission profiles. To capture production uncertainties, small variations in system parameters are introduced. A Monte Carlo simulation is employed to evaluate the robustness of the optimized solutions.

2. Digital-Twin verification:

Detailed Digital-Twin simulations are conducted to verify the optimized ESS designs. These simulations incorporate developments from all WPs (semi solid state and supercapacitor models, energy management-PMS/EMS, AC/DC architecture for components integration), providing a high-fidelity validation environment.

The comparative analysis of performance, fuel efficiency, and greenhouse gas (GHG) emissions serves to validate and confirm the viability of the pre-designed ESS concepts.

In summary, Deliverable D2.4 demonstrates the robustness, efficiency, and environmental benefits of the optimized ESS designs through advanced digital twin simulations—marking a key step towards reliable, low-emission hybrid energy systems within the AENEAS project.

Attainment of the objectives and explanation of deviations

Due to the low technology readiness level of solid-state battery (SSB), system-level design and prototyping proved challenging, raising doubts about the feasibility of achieving a TRL7 onboard demonstration in the near future (by 2027). As a result, and with the agreement of both the consortium and the project officer, the project strategically shifted its focus to semi-solid-state battery (SSSB) technology at the system level, which offers a more mature and practical pathway toward onboard demonstration. Consequently, this deliverable integrates SSSB technology into the ship-level simulations.

2.1 Overall methodology

The methodology of D2.4 relies on a modeling approach that executes multiple simulations to evaluate at the complete ship level and under real-sailing and variable conditions the viability of the AENEAS new designs with respect to criteria of fuel consumption and CO₂ emissions performance. This is the first attempt within AENEAS that the developed solutions are integrated and tested on an entire ship, even if this is accomplished in a virtual test-bed environment rather than a real one.

The chain that is followed to achieve targets combines three main pillars that are visualized in Figure 1, while their role is briefly explained in the following paragraphs.

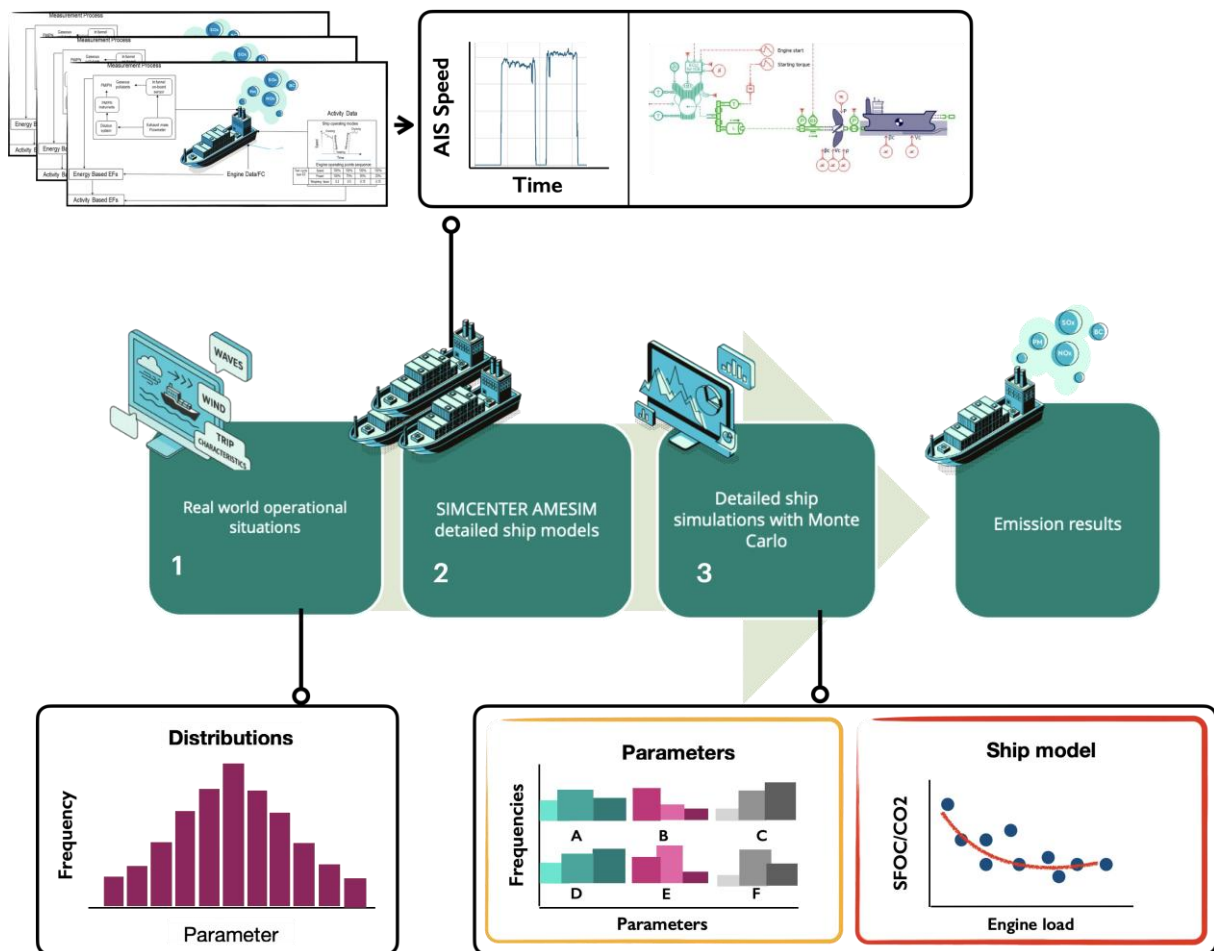


Figure 1. Methodological chain with tools and processes displayed in three main pillars

- I. The **first pillar** intends to specify and numerically describe the **operational situations** that the ships face during their real-world activity to evaluate whether the new designs remain effective under a wide spectrum (normal and extreme) sailing conditions and operating events. Parameters that may affect performance are climatic conditions, trip characteristics and design-related specifications. A critical process within this pillar is to accumulate realistic data for these parameters and organize them in a way that will reflect the variability that they present within an entire year of ship operation.
- II. The **second pillar** includes **ship powertrain models** that undertake the role of the offline digital representations of the actual ships in the three use-cases. The ship modes

that have been developed in previous AENEAS Tasks (Tasks 2.1 & 2.2) are updated here with the inclusion of the new ESS (SSSB, supercapacitors) and with the optimization of the energy management strategy achieved in Task 2.3. The models are also parametrized here with actual ship geometric characteristics to obtain a more physical background that is necessary for the needs of an analysis that tries to approach as much as possible the reality of sailing conditions.

- III. The **third pillar** is the actual **execution of simulations** with the powertrain model being fed with the variable operating parameters to quantify the energy and CO₂ emissions performance of the examined electrified ships under the new design. Given the increased number of parameters and their variability in real world, a Monte Carlo approach is used to combine them reasonably, taking account the likelihood of their occurrence during the ship real-world operation.

The following sections describe in detail the various tools and methods as well as explain the adaptations that were made within this Task.

2.2 Ship-powertrain models

2.2.1 Modeling background in the platform of Simcenter Amesim

The platform of Simcenter Amesim [1] is used to compile the detailed ship model that is the main pillar of the evaluation chain to characterize the vessel's performance. The model in Simcenter Amesim is categorized as an instantaneous power-based one. In this modeling category, the equations solved to calculate the various numerical parameters have a physical background mainly based on the power that is required for the ship movement. Such power is requested by the propeller and is produced by the engine. The term instantaneous refers to the second-by-second time resolution at which these estimations are provided.

In this context, the instantaneous power demand of the ship is determined by the fundamental mechanical relationship:

$$P = R_{\text{total}} \times V \quad (1)$$

where P is the propulsion power at the propeller, R_{total} is the total resistance force acting on the ship and V is the instantaneous vessel speed. In particular, the resistance R_{total} , i.e. the total force that must be overcome by the propulsion system to maintain or change speed, is a combination of three main forces and it is calculated with the following expression:

$$R_{\text{total}} = R_F + R_W + R_A \quad (2)$$

where the term R_F represents frictional resistance, R_W is the wave-making and R_A represents the air resistance effects.

Consequently, the product of total resistance and the vessel velocity provide the instantaneous mechanical power required at the propeller to counteract these resistive forces. This formulation allows the model to compute on a second-by-second basis the evolving power demand profile of the ship under varying operating conditions. Then, the power that has to be produced by the engine to cover this demand is then calculated taking account the various losses at the propulsion chain of the ship starting from the propeller, passing through a transmission component (gearbox/final drive) as transferred through the shafts and concluding back to the engine with the following relationship:

$$P_{\text{eng}} = P \times \eta \quad (3)$$

where P_{eng} refers to the power produced by the engine at the shaft, P is the propulsion power at the propeller and η represents the overall efficiency of the ship's mechanical powertrain, from the engine to the propeller.

The various ship components of the powertrain through which power flows are represented with sub-models, and the overall ship model is compiled by connecting them with mechanical, electrical, and signal links. The following bullet points summarize the principles behind the various components as well as their main outcomes that are important for the targets of this Deliverable.

- The internal combustion engine components (main and auxiliary engines) produce the mechanical power demanded by taking into account the losses during fuel combustion.

The main engine does not only produce power for propulsion but also to cover the auxiliaries needs. Auxiliary engines on the other hand only produce power to generate electricity in gensets. Nevertheless, the rationale is the same with this component taking into account the losses from converting fuel energy to mechanical. The equation that associates power production with fuel consumption is the following where the energy transformation efficiency is described by the specific fuel consumption term (SFOC) which is variable depending on the engine load and described by a map in the model.

$$FC = P_{eng} \times SFOC \quad (4)$$

- The electric machines (motor/generator/inverter/shaft generators) are also modelled by an equivalent circuit (current source), Conversion losses between electrical and mechanical power, for both motoring and generating operation, are accounted for through a constant efficiency factor (n), applied uniformly and independent of rotational speed and torque.

$$P_{el,gen} = P_{mech} \times n \quad (5)$$

$$P_{mech} = P_{el,cons} \times n \quad (6)$$

- The energy storage components of (battery and supercapacitor packs) are modelled through an equivalent circuit representation (RC battery model), consisting of an open-circuit voltage source in series with internal resistances and one or more RC branches to capture transient polarization effects. In this representation, the instantaneous electrical power exchanged with the ship's power bus is computed as:

$$P = V_{term} \times I \quad (7)$$

where V_{term} represents the terminal voltage of the battery, and I the current (negative during discharge and positive during charge). The terminal voltage is expressed as:

$$V_{term} = V_{OCV} - IR_{int} - \sum_k V_{RC,k} \quad (8)$$

All these parameters, the open-circuit voltage, internal resistance, and RC branch elements are functions of the battery's state of charge (SOC) and battery temperature (T). This dependency allows the model to reproduce close to electrochemical behavior under varying operating conditions, capturing both efficiency degradation and dynamic response. As a result, the RC model provides a physically consistent, time-resolved estimation of the instantaneous power demand or supply, enabling detailed analysis of the energy flow and performance of the overall propulsion and energy management system.

- For the energy management strategy of the hybrid powertrain, a control unit converts the load requests (for ship propulsion and auxiliaries' needs) to engine control signals. A control unit also implements the energy management logic (ruled based) which decides how the power is split between the two energy carriers (fuel and electricity) affecting the operating points of the various engines (ME & AE).

A more detailed resistance model for AENEAS needs

A special mention should be made on the ship resistance model. In this study, ship resistances are calculated with the Holtrop & Mennen (H&M) method to provide a more physical dimension in the analysis. The Holtrop and Mennen method is an empirical, regression-based approach for predicting a ship’s total resistance. Resistance is broken down into individual components, such as frictional, form, wave-making, appendage, and bulbous bow resistance, each derived from extensive data across a wide range of hull forms. The total calm water resistance is computed as the sum of several components representing different physical effects. This is more analytical than the eq.2 that provided more generic resistances categorization.

$$R_{Total} = R_F(1 + k1) + R_{APP} + R_W + R_A + R_{TR} \tag{9}$$

In the Holtrop–Mennen method, R_F represents the frictional resistance, where $1 + k1$ is the form factor describing the viscous resistance of the hull form in relation to R_F , R_{APP} is the appendage resistance, R_W is the wave-making resistance, R_B is the additional resistance due to the bulbous bow, and R_{TR} is the additional resistance due to the transom stern. R_A represents the skin friction and air resistance effects, considering the correlation between the model scale and full scale. Detailed formulations and empirical coefficients for each component are provided in the original Holtrop–Mennen papers [2].

Given basic geometric inputs (ship length, beam, draft, block coefficient, wetted surface area, etc.), the method estimates the effective power and resistance curve over speed design, and the water and wind conditions. The most important parameters utilized in the Holtrop–Mennen method are described in Table 1 along with their symbols. The following sections provide more information on how parameters are calculated.

Table 1 Key parameters of the Holtrop & Mennen ship resistance prediction method

Symbol	Description
L_{WL}	Waterline length
B_{WL}	Breath
T_a	Afterward Draft
T_f	Forward Draft
∇	Volumetric Displacement
S	Normal section shape
C_B	Block coefficient
C_M	Midship coefficient
C_P	Prismatic coefficient
C_{WP}	Waterplane coefficient
$1 + k1$	Form factor

Symbol	Description
A_{bt}	Transverse bulb area
h_b	Center of bulb
A_t	Transom area
V	Ship speed

Hydrostatic Coefficients Estimation Under Varying Load-Displacement

To evaluate the variation of the main hull-form coefficients with respect to the ship's displacement, an iterative computational approach was implemented. The method computes the draft and updates hydrostatic coefficients, block coefficient, midship coefficient, prismatic coefficient and waterplane coefficient for any given displacement conditions.

It is important to note that Simcenter Amesim does not update the ship's geometric and hydrostatic parameters automatically as loading changes. Amesim uses the coefficients provided at the reference design point. Therefore, for every off-design loading condition (i.e. different displacement), the hull coefficients must first be recomputed externally in a MATLAB script (summary of calculations are provided below), and then the updated parameters must be manually reintroduced into the Amesim model for that specific loading scenario.

Draft change

At each iteration, the ship draft is updated according to the hydrostatic relation between displacement and waterplane area. The draft (T) represents how deeply the ship sits in the water. As the displacement weight (w) changes (due to cargo, fuel, etc.), the ship must displace an equal volume of water to maintain hydrostatic equilibrium:

$$\Delta \nabla = \frac{w}{\rho} \quad (10)$$

For a small sinkage, the extra displaced volume can be approximated as prismatic volume defined by a base equal to the waterplane area and thickness equal to the draft change ΔT .

$$\Delta \nabla = A_{wp} * \Delta T = C_{WP} * L * B \quad (11)$$

The waterplane area A_{wp} is the planform area of the ship's hull at the waterline:

- C_{WP} : Waterplane area coefficient (dimensionless),
- L_{WL} : length at the waterline (m),
- B_{WL} : breadth at the waterline (m).

By solving for the draft change, we get the following relation:

$$\Delta T = \frac{\Delta \nabla}{A_{wp}} \Leftrightarrow T = T_0 + \frac{V - V_0}{A_{wp}} \quad (12)$$

The waterplane area A_{WP} depends on the waterplane coefficient C_{WP} which in turn varies with the block coefficient C_B . The coupling between these parameters is resolved iteratively until convergence.

Assumptions and simplifications on the above formulas:

- In the above method, L_{WL} and B_{WL} parameters remain constant, and all displacement-related changes are reflected through the variation of T (draft) and the derived hydrostatic coefficients.
- In this analysis, the forward and afterdrafts are assumed to be equal, implying a zero-trim condition. This simplification allows the vessel to be treated as operating on an even keel, ensuring that variations in displacement affect only the mean draft and not the trim angle. Consequently, the recalculated hydrostatic and form coefficients correspond to symmetric loading conditions.

Geometrical Coefficients Formulations

The block coefficient quantifies how full or fine the underwater hull shape is, by comparing the actual displacement volume of the ship to the volume of an imaginary rectangular block that encloses it. Assuming constant length and beam values for small draft changes the new block coefficient at each displacement condition can be derived as:

$$C_B = \frac{\nabla}{L_{WL} B_{WL} T_{new}} \quad (13)$$

Both the midship coefficient C_M and the waterplane coefficient C_{WP} are empirically linked to the block coefficient, ensuring geometry consistency as the hull's displacement and thus its overall fullness changes.

The midship area coefficient was estimated with Kerlen method [3]:

$$C_M = 1.006 - 0.0056 C_B^{-3.56} \quad (14)$$

This coefficient represents the fullness of the ship's midship underwater section relative to a rectangle with the same breadth and draft. A higher C_M indicates a fuller, more rectangular midship shape, while a lower value corresponds to a finer hull form.

To estimate the waterplane area coefficient, Parson method was used [4]:

$$C_{WP} = \frac{C_B}{0.471 + 0.551C_B} \quad (15)$$

This coefficient expresses how large the ship's waterline area is compared to its enclosing rectangle $L \times B$. It reflects the vessel's stability and overall buoyancy in the water.

Both Kerlen and Parson relations, are regression-based fits derived from large ships form data.

The prismatic coefficient is linked to the block and midship coefficients via the relation:

$$C_P = \frac{C_B}{C_M} \quad (16)$$

It represents the longitudinal distribution of the underwater volume along the ship's length. A higher C_P indicates that the volume is more evenly distributed (full-bodied hulls such as

tankers or bulk carriers), while a lower C_p corresponds to a more tapered form with finer ends (typical of high-speed vessels).

Additional geometric parameters such as the bulbous bow area, bulb height and transom area are scaled proportionally to the draft ratio based on the following relation:

$$\Phi = \frac{T}{T_0} \Phi \quad (17)$$

Where:

- Φ represents each parameter.
- T is the new draft calculated by eq.12
- T_0 is the draft at the vessel design point which is known by vessel datasheet.

2.2.2 Ship models (baseline & AENEAS integrations) for Use-Case 1

This part of D2.4 describes the ship models that are developed to describe the baseline ship of Use Case 1 (reflecting the situation before AENEAS), as well as the ship after the integration of the AENEAS solutions.

2.2.2.1 Baseline ship model

The baseline model of use-case 1 before the integration of AENEAS solutions is presented under this section. Elements from previous WP2 tasks are summarized and necessary updates conducted in this Task are highlighted.

- **General characteristics and topology**

A hybrid short-sea Ro-Ro vessel operating on the Genova-Livorno-Catania route (based on Grimaldi delivered ship recordings) is examined in this use-case 1 evaluation. This ship is a roll-on/roll-off ship designed to carry wheeled cargo, such as cars, motorcycles, trucks, semi-trailer trucks, buses, trailers, and railroad cars. Its total capacity is over 500 trailers. AENEAS retrofits the ship advancing its battery system and the energy management strategy still aims to ensure the provision of the necessary electrical power during port stays, enabling operations with as low emissions as technically possible while in port.

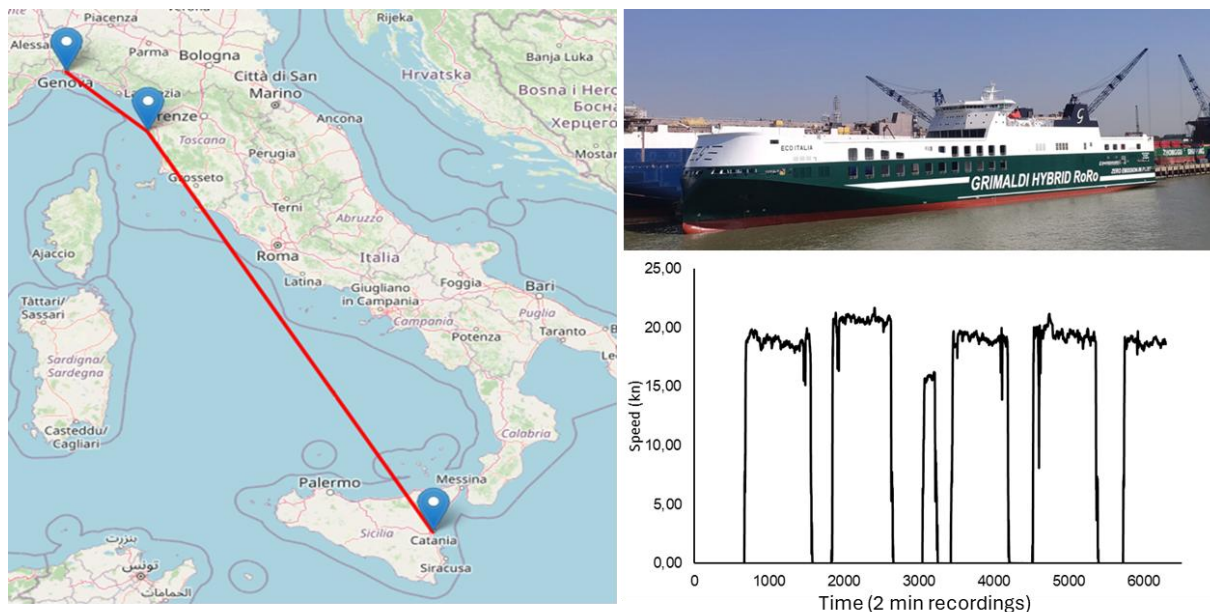


Figure 1 Example route of the Grimaldi RO-RO vessel used in the Amesim simulation

The vessel follows the typical ship operational cycle characterized by sequential port-stay, maneuvering, and navigation phases that are common in all ship types. The representative travel analyzed in this study is depicted in Figure 1 in terms of its speed profile and contains an average port stay of 11,5 hours (max 22 hours, min 5 hours), a mean cruising speed of 19 knots with an average duration of 22 hours, and an average maneuvering duration of 1,2 hours (acceleration and deceleration phases accounted together).

The examined vessel is equipped with two slow-speed internal combustion (IC) main engines (ME), each rated at 13 MW, which provide propulsion during navigation and maneuvering. Mounted on the ME shafts are two generators, which convert part of the mechanical energy produced by the ME into electricity to meet the vessel's auxiliary power demands during navigation and maneuvering phases.

For additional auxiliary power, the vessel is fitted with three high-speed IC auxiliary engines (AE), each rated at 1,5 MW, which drive gensets to produce electricity. These AE operate only during maneuvering and in-port stay, progressively assuming the role of supplying auxiliary power from the ME as the ship approaches port. Specifically, two of the AE power bow thrusters used for ship maneuvers, while the third supplies the hotel load during port operations.

The hybrid system is supplemented by 4 battery banks with a total capacity of 4,9 MWh for energy storage. The size of the energy storage system has been configured in previous tasks based on the total energy needed during maneuvering and port stay. The batteries are charged during navigation and maneuvering via the ME shaft generators and are discharged during port stays to cover hoteling consumption.

The architecture summary of this use-case is given by:

- Main engines: 2 x 12780 kW (@ 117 rpm, Tier II)
- Shaft generators: 2 x 2000 kW
- Bow thrusters: 2 x 2000 kW
- Diesel generators: 3 x 1540 kW (@1000 rpm, runs on HFO & MGO)
- Battery packs: 4 x 1225kWh

Figure 2 provides a schematic representation of how this ship powertrain topology was represented with a model in the platform of Simcenter Amesim. Layout of Figure 2 also shows the various components along with their connection with mechanical, electrical and signal links that shape when combined the complete powertrain of the hybrid ship.

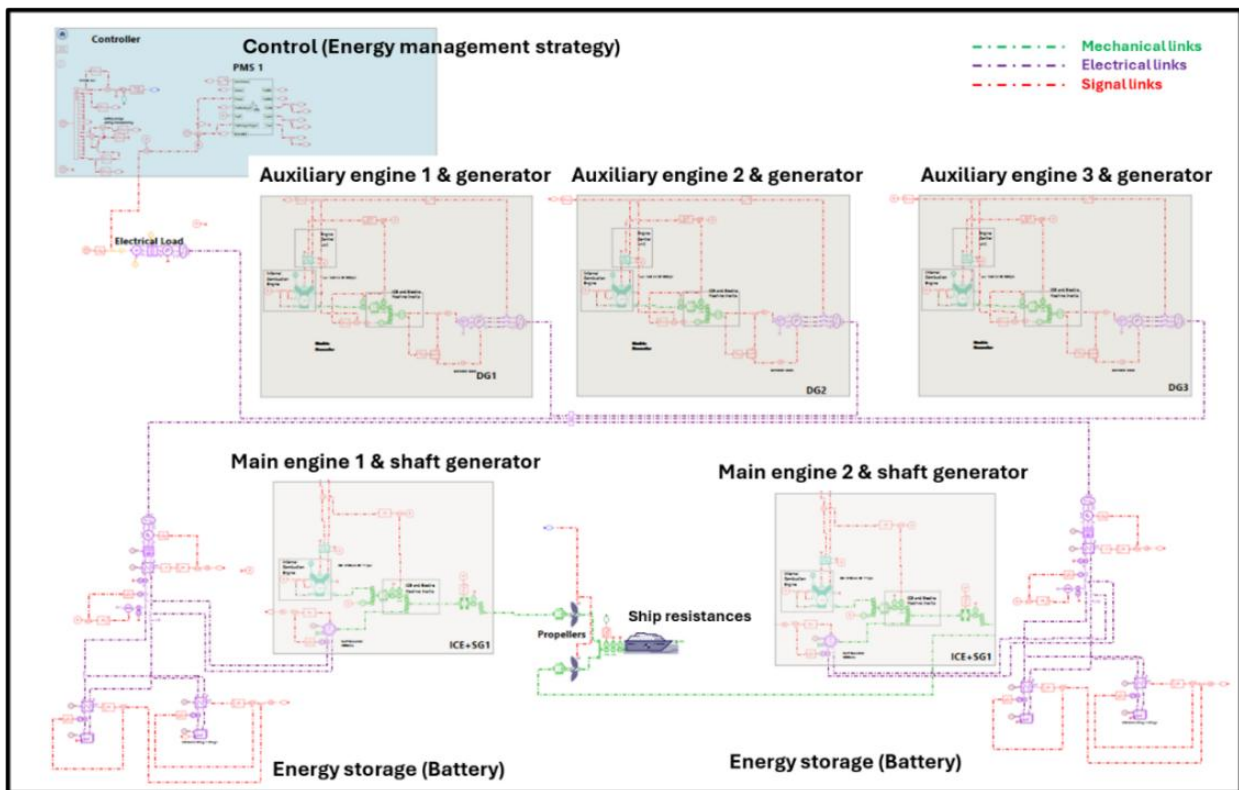


Figure 2 Hybrid Ro-Ro ship powertrain topology as modeled in Simcenter Amesim

- **Baseline energy management strategy**

The previous presentation of the powertrain layout and the synergies between its components also illustrates the fundamental energy management strategy applied in the hybrid vessel. The ship aims to achieve close to zero-emission operation during port-stay, which is accomplished by utilizing the batteries instead of the auxiliary engines until their charge is depleted. Consequently, the batteries must be fully charged before the vessel reaches the port. To ensure this, excess energy is generated during navigation by operating the ME at a higher load point compared to a similar vessel without battery systems. This behavior is illustrated in the left panel of Figure 3, where actual average ME load recordings from the hybrid vessel are compared with a theoretical scenario in which no battery charging would occur from the main engine. The theoretical case was derived by subtracting the battery charging profile from the main engine power output.

Figure 3 also presents the second and most important element of the energy management strategy, the deactivation of AE operation during parts of port-stay because of the presence of the battery system. The blue line in the Figure 3 again represents the theoretical case where AEs would operate fully if batteries did not exist.

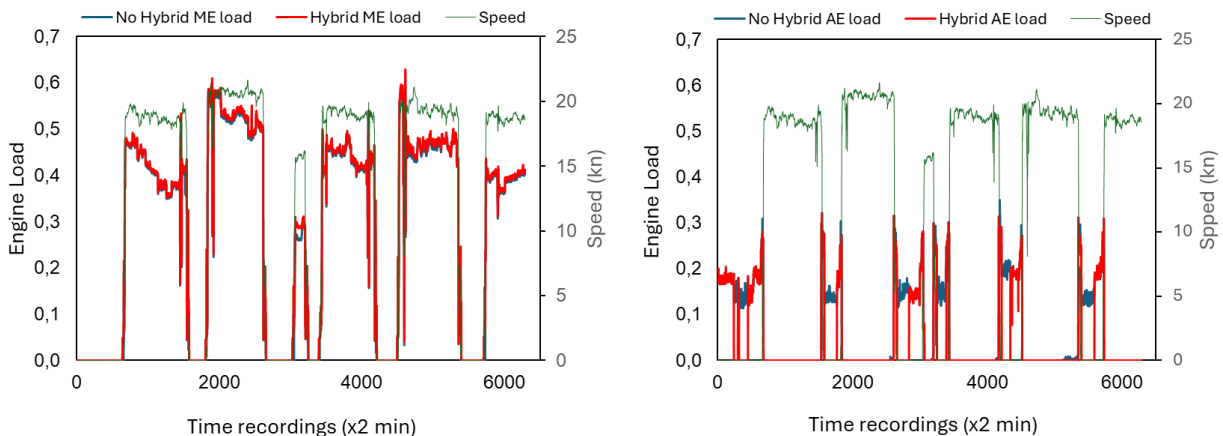


Figure 3 MEs (left) and AEs (left) average operating load for the hybrid (red) and a non-hybrid similar ship (blue)

Overall, this strategy leverages the larger and more energy-efficient ME to operate closer to their optimal specific fuel consumption range during cruising, while simultaneously charging the batteries. The stored energy is then used during port stays to supply auxiliary power, thereby relieving the less efficient auxiliary engines from this task. As a result, the system achieves the main target which is the close to zero-emission port operation through battery-supported and engine-off hoteling, while also ensuring an efficiency in terms of fuel consumption operation for the entire trip.

- **Model re-parametrization**

Within this task, the baseline ship model in Simcenter Amesim for use-case 1 was re-parameterized using the vessel's actual geometric characteristics. This adjustment was necessary to enable an accurate performance analysis under varying environmental conditions - such as wave height, wind speed, and other external factors, that influence the total resistance the ship must overcome during operation.

Preliminary models developed in earlier tasks employed more generic resistance estimation methods that were not sensitive to such input variations. To address this limitation as previously mentioned, the Holtrop and Mennen method was adopted as a suitable approach for modeling air, wave-making, and viscous resistance components. This method offers the desirable function but requires a detailed geometric description of the vessel to perform the necessary calculations. So, the basic geometric parameters of the ship were updated in the model with the values that are presented in Table 1.

Only the main dimensions and displacement were available in deliverable D1.1, with no CAD model of the hull. With fewer data and no CAD model, inserting accurate geometric parameters requires making some estimations. Since main dimensions and displacement were available, the block coefficient could be calculated based on the equations of section 3.2.1. For the midship area coefficient and waterplane area coefficient, estimation methods commonly used at preliminary design stages can be applied. The prismatic coefficient can be easily obtained as it is the ratio of the block coefficient to the midship area coefficient. Refer to the relevant introductory section where information for the calculation method is provided to define the missing parameters.

Table 2 Ro-Ro ship geometric characteristics necessary for the Holtrop and Mennen method (use case 1).

Ship Parameters	Value	Unit	Source
Nominal Mass	37336	tones	Deliverable D1.1
Length	238	m	Deliverable D1.1
Waterline length	229.75	m	Deliverable D1.1
Draft	7.2	m	Deliverable D1.1
Breadth	34	m	Deliverable D1.1
Transverse bulb area	20	m ²	Assumption*
Center of bulb area	3	m	Assumption*
CB (nominal)	0.6476	-	Calculated
CP (nominal)	0.6611	-	Calculated
CM (nominal)	0.9797	-	Calculated
CWP (nominal)	0.7823	-	Calculated

* Assumption based on vessel of similar category

The above values have been calculated for the design loading point of 37,336 metric tons. For different loading points the recalculation process for the geometric coefficient takes place.

- **Model re-validation**

After the new parameterization, a re-validation process was evidently needed to test the accuracy of the model. The experimental recordings from the actual trip on engine power output and on battery SOC were used and compared with the estimations provided by the model when this was fed only with the speed profile of the trip. Figure 4 provides this comparison for the variable of the ME power output on the left side and for the battery SOC on the right one. It is noted that these two variables were selected being important for an analysis that evaluates the performance of an electrified powertrain, covering two of the most critical components of this hybrid configuration – the ICE engine to represent the mechanical performance and the battery to reflect the electrification behavior.

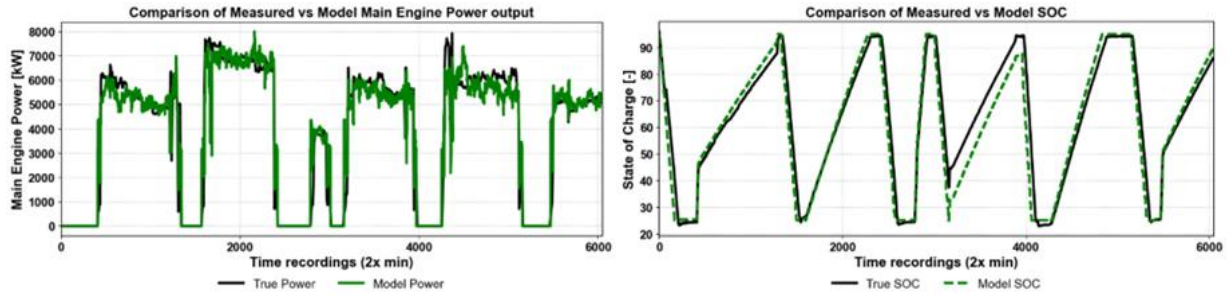


Figure 4 Model validation comparing actual recordings with model estimations for ME power (left) and battery SOC (right).

As is evident from Figure 4, the model predictions present good agreement with the actual recordings for both examined variables, which means that the model is validated and can be adapted to the AENEAS solutions for performing their evaluation.

2.2.2.2 Ship model after AENEAS solutions integration

Previous descriptions concerned the baseline ship topology consisted of the default energy management strategy and the conventional NMC battery chemistry with the liquified electrolyte. This section focuses on the adjustments made in the model to achieve the integration of the new storage technology and the compilation of the energy management strategy.

- **Ship topology new characteristics after AENEAS**

Table 3 summarizes the new characteristics of the ship topology. The battery sizing remained the same while electrolyte chemistry is the main parameter that changes by replacing the liquefied material with the semi-solid one. The number and the way that battery cells are connected to formulate the battery package are also depicted in Table 3 showing small differences between the previous and the new pack design layout. The new battery in AENEAS has however a higher gravimetric density, meaning that more free space and less weight can be ensured for the examined ship with the new design.

Table 3 New vs old Ro-Ro ship topology modifications (use case 1).

Parameter	Baseline model	Model after AENEAS
Cell Type	Lithium-ion	Semi Solid State
Cell Capacity [Ah]	69	107
Number of battery packs	4	4
Num of cells in series	266	268
Num of cells in parallel	18	12
Total Pack energy [kWh]	~ 5000	~ 5000
Energy density-gravimetric [Wh/kg]	>200	>300
Energy management strategy	Rule based	Optimized rule-based

- **New energy management strategy**

A new optimized rule-based strategy for use-case 1 was implemented in the model based on the ECMS developed in Task 2.3, which however hadn't been applied previously to the ship

model. This new strategy mainly differs from the baseline strategy regarding the optimization of the maneuvering phases of acceleration and deceleration with a better exploitation of the ME instead of the AE for the auxiliaries need coverage. In particular, the strategy seeks to:

- cover from the ME all the auxiliaries need during maneuvering as far as this is possible, including bow trusters keeping the AE out of operation. This requires operating the ME to a higher and more efficient load point to produce this excess electrical power for auxiliaries. This also means that the battery charging during the maneuvering is avoided and is implemented only in cruising. The latter is a differentiation from the previous strategy.
- operate the AEs at high efficiency point, adapting their operation to the instantaneous electrical demand. When possible, only a single AE is kept active to cover the load, thereby avoiding inefficient partial-load operation across multiple engines.

Apart from these two targeted modifications, the overall structure of the optimized strategy remains consistent with the base configuration, maintaining the same propulsion and energy-management architecture while enhancing its operational logic through refined rule-based coordination. Figure 5 shows a snapshot of the impact on the SOC of the optimized vs the previous strategy during the acceleration phase.

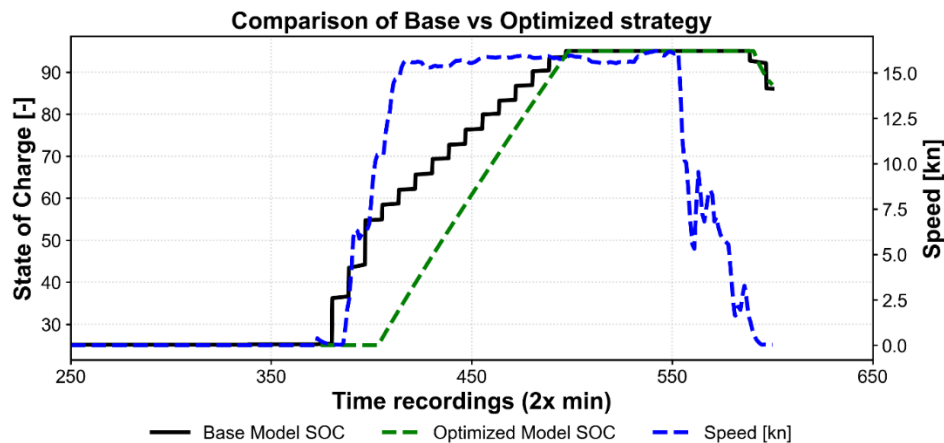


Figure 5 Figure showcasing the optimized battery charging strategy: avoiding charge during port or maneuvering phase.

2.2.3 Ship models (baseline & AENEAS integrations) for use-case 2

This part of D2.4 describes the ship models that are developed to describe the baseline ship of Use Case 2 reflecting the situation before AENEAS as well as the ship after the integration of the AENEAS solutions.

2.2.3.1 Baseline mode

- **General characteristics and topology**

The second use-case is a Ro-Pax ship that transfers vehicles, cargo and passengers during its operation on the route linking Civitavecchia, Italy to Barcelona, Spain via Porto Torres (Sardinia). This case studies a bigger ship on a longer route compared to the first case.

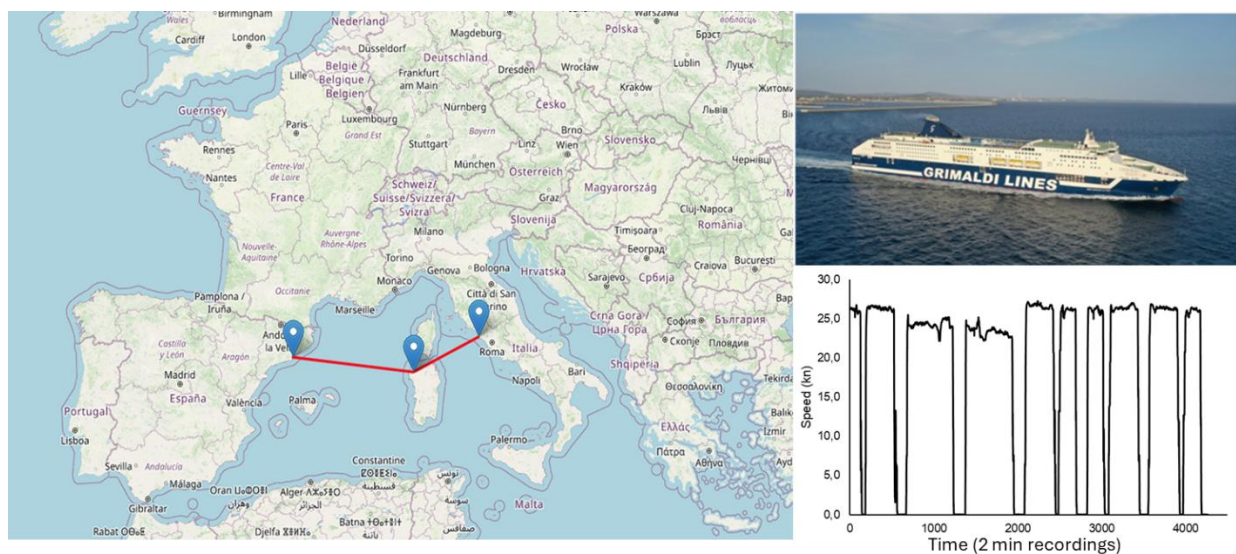


Figure 6 Example route of the Grimaldi RO-PAX vessel used in the Amesim simulation

This ship, like use-case 1, follows the typical trip sequence of port-stay, acceleration, cruising, deceleration, port-stay. The specific trip statistics indicate that the average cruising speed is found at 25,3 kn, being 32% higher than use-case 1. Such increased speed is a reasonable observation considering that the ship sails in a more open-sea environment linking two different Mediterranean countries. The mean maneuvering time is 39 minutes per acceleration and deceleration phase (54 minutes considering both acceleration and deceleration together as maneuvering), like the first use case, while the port stay has much less duration than use-case 1, accounting for 2.8 hours on average compared to the more extended period of 11 hours of use-case 1.

The total installed power of the MEs is double compared to the use-case 1 (56 vs 26 MW) and it is achieved by combining four ME of 14 MW each, instead of two engines of similar capacity that are installed at the previously examined Ro-Ro ship. The installed capacity for auxiliaries' coverage is also increased, rated at 6,7 MW and achieved by combining three AE of 2,2 MW. This ship is again a hybrid one, equipped with shaft generators mounted at the ME as well as with a battery of 5,5 MWh of total capacity, which is slightly increased compared to use-case 1.

The representation of the ship model in Simcenter Amesim is provided in the following figure. The layout is similar to use-case 1 with the main difference related to the inclusion of two additional main engines that are organized in two blocks consisting of two engines each. The architecture summary of this use-case, as shown in Figure 7, is given by:

- Main engines: 4 x 13860 kW
- Shaft generators: 2 x 2300 kW
- Bow thrusters: 2 x 1850 kW
- Diesel generators: 3 x 2550 kW
- Batteries: 2 x 2735 kWh

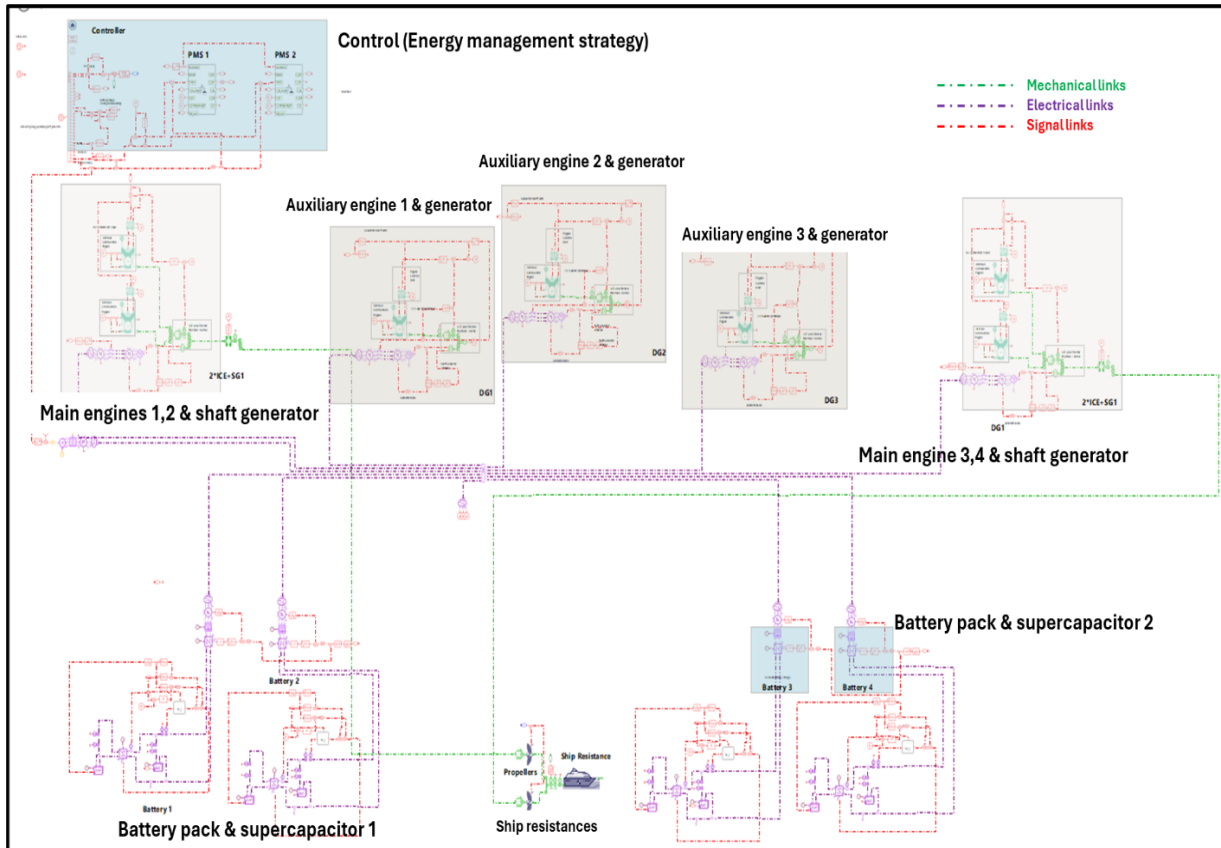


Figure 7 Hybrid Ro-Pax ship powertrain topology as modeled in Simcenter Amesim

- **Baseline energy management strategy**

The energy management strategy of the baseline ship model in use-case 2 shows several similarities to that of use-case 1, but also some differences. These arise primarily because the vessel examined here is of a different and larger type, with correspondingly higher energy requirements. Additional variations stem from the specific trip analyzed, during which the vessel altered its behavior in certain segments due to external or unknown factors. These deviations represent situational adjustments rather than fundamental changes in the underlying energy management logic.

In this configuration, the MEs provide propulsion and supply auxiliary electrical power during cruising and maneuvering via the shaft generator. However, this pattern presents some deviations within the trip that constitutes a difference from use case1. In case 1, the MEs using the shaft generators covered all auxiliary loads during cruising and maneuvering (except for bow thrusters) throughout the entire activity profile. In the present case study, there are instances where the MEs supply a portion of the auxiliary demand during certain cruising segments. Consequently in these instances, the AEs operate in parallel with the ME during some cruising periods to cover the remaining load. These instances occur when the shaft generators mounted on the MEs are fully or partially deactivated. Nevertheless, there are also

cruising intervals where the MEs once again cover the full auxiliary demand, confirming the dominance of the intended operating strategy observed in use case 1.

As in use-case 1, the MEs charged the battery via the shaft generator during cruising and maneuvering. However, when the shaft generators are inactive, battery charging is carried out by an AE, which simultaneously supplies the remaining electrical consumers during cruising. When the battery reaches full charge before the vessel arrives at port, deceleration charging is not activated.

The AEs supply electrical power during port operations where the MEs are shut down. They also operate during maneuvering to power the bow thrusters and—as noted—during certain cruising and maneuvering intervals to cover part of the auxiliary demand. The vessel is equipped with three AEs to ensure that these requirements can be met.

During port stays, the battery substitutes for one of the AEs for as long as sufficient charge is available. Once the battery is depleted, an AE resumes supplying hotel and auxiliary loads.

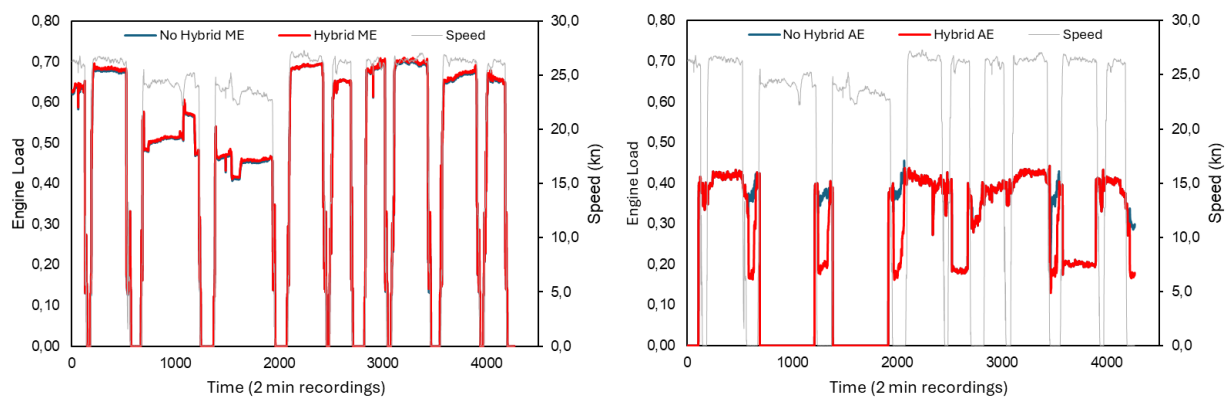


Figure 8 MEs (left) and AEs (right) average operating load for the hybrid (red) and a non-hybrid similar ship (blue)

The overall hybridization strategy is illustrated in Figure 8, which shows that the MEs operate at a slightly higher load point in the hybrid configuration to charge the battery, compared with a conventional vessel of similar type.

The AE panel in Figure 8 highlights two key observations. First, the AEs operate during certain cruising segments to supply the auxiliary load—unlike in use-case 1, where they remained completely inactive throughout all cruising periods. Periods in which the AEs are partially or fully shut down during cruising are also present. There, auxiliaries are covered partially or fully by the ME through the shaft generator

Second, although the battery reduces the operation of AE during port stays, it does not eliminate it entirely. One AE remains active to cover part of the hoteling load. In contrast to use-case 1—where some port-stay intervals were entirely emission-free—the present case always involves at least one operating AE. Nonetheless, hybridization reduces the number of AEs required during port operations, which becomes particularly evident when the batteries are not used, and additional AEs are needed to meet the associated load.

- **Model re-parametrization**

As it became evident from use-case 1, the type of analysis conducted here requires a physics-based model that is parametrized with the actual ship geometrical characteristics. This Task

adapted the models of Simcenter Amesim in this direction, with the parameters used to model the Ro-Pax ship of use-case 2 being presented in the following Table.

Table 4 Ro-Pax ship geometric characteristics necessary for the Holtrop and Mennen method (use case 2).

Ship Parameters	Value	Unit	Source
Nominal Mass	33830	tones	Deliverable D1.1
Length	253.8	m	Deliverable D1.1
Waterline length	231.62	m	Deliverable D1.1
Draft	7.2	m	Deliverable D1.1
Breadth	30.4	m	Deliverable D1.1
Transverse bulb area	20	m ²	Assumption*
Center of bulb area	3	m	Assumption*
CB	0.651	-	Calculated
CP	0.6642	-	Calculated
CM	0.9802	-	Calculated
CWP	0.7846	-	Calculated

Again, the values of the geometric coefficients have been calculated at the reference loading point.

- **Model re-validation**

Similar to use case 1, a re-validation of the model was conducted given that the ship model was adapted to its actual parameters. The ME power outputs of recordings vs the simulations are provided in Figure 9.

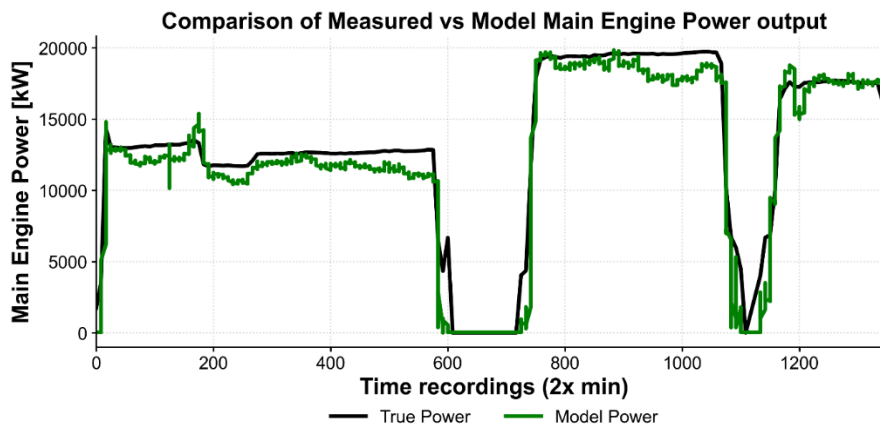


Figure 9 Comparison of main engine power between model and recordings.

The recorded power curve appears relatively flat in many regions of the trip, and this is simply a consequence of the low sampling frequency of the experimental dataset. For this reason, short time fluctuations are not captured. Nevertheless, the comparison clearly shows that the model reproduces the correct magnitude and overall trend of the main engine power output across all operating regions of the above trip.

2.2.3.2 Ship model after AENEAS solutions integration

- **Ship topology new characteristics**

AENEAS in use-case 2 focuses on retrofitting the Ro-Pax ship with an additional level of hybridization. So, in this use-case, there isn't a replacement in battery chemistry as in use-case 1, which is kept the same with the initial design. What is changed here is the addition of a supercapacitor in the hybrid system of the ship that works in parallel with the battery, particularly focusing on covering the transient operation during the maneuvering trip phases.

The new topology characteristics of the use-case 2 are summarized in the following table, that shows the changes and additions in the energy storage system of the hybrid ship, along with the implementation of a new energy management strategy.

Table 5 New vs old Ro-Pax ship topology modifications (use case 2).

Parameter	Parameter	Baseline model	Model after AENEAS
Battery	Cell Type	Lithium ion	Lithium ion
	Cell Capacity [Ah]	69	69
	Number of battery packs	4	4
	Num of cells in series	266	266
	Num of cells in parallel	18	18
	Total Pack energy [kWh]	~ 5000	~ 5000
	Energy density-gravimetric [Wh/kg]	>200	>200
Supercapacitor	Capacity [F]	-	3000
	Min Voltage [V]	-	0
	Max Voltage [V]	-	2.7
	Energy Density [Wh/kg]	-	5.6
	Pack Total Energy [kWh]	-	38 kwh
	Pack Total Power [kW]	-	2 MW
Energy management strategy	Energy management strategy	Rule based	Optimized rule-based

- **New energy management strategy**

The new energy management strategy intends to cover the maneuvering phases of the trip as it handles the AE peaks with the hybrid energy storage system. In particular.

- SC is used to this process in combination with an AE to achieve a more stable operation of the latter during the maneuvering phase, as seen Figure 10. When the SC state of charge (SOC) reaches its upper limit, any excess energy produced by the DGs is redirected to the battery pack. This behavior is clearly illustrated in the second maneuvering phase of Figure 11, where the battery power is negative (charging) and no power is provided or absorbed by the SC.
- The battery is aggressively charged (negative power) before reaching the port if the SOC was not as high as possible, to exploit the maximum of its SOC window potential

during the port stay, Figure 12. During port stay the battery is discharging until minimum SOC is reached. Afterwards, DGs operate to cover the electrical needs of the vessel. No SC usage during this phase.

- During the navigation phase, supercapacitor modules slowly discharge to the battery, so that their SOC stays at the desired level of 50%.

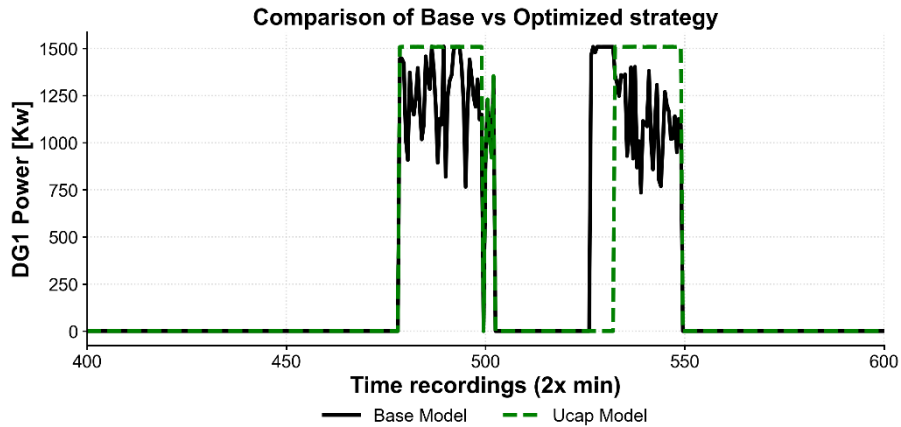


Figure 10 Peak Shaving strategy for DG1 using the Supercapacitors during the maneuvering (acceleration and deceleration between one port stay).

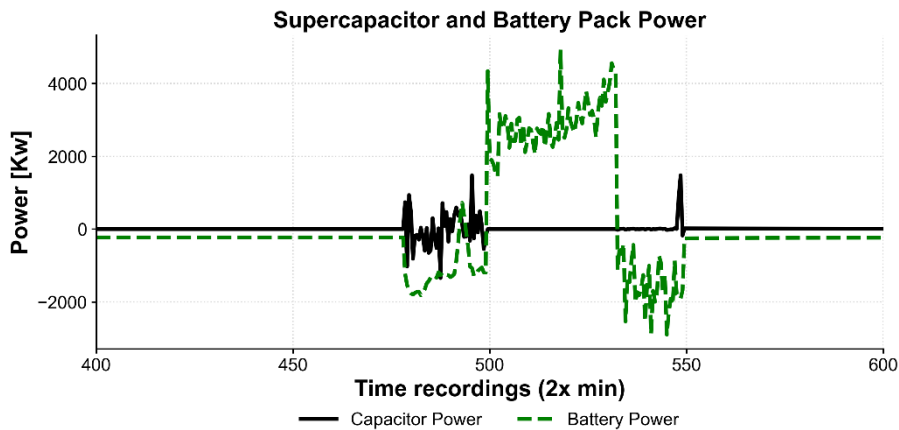


Figure 11 Supercapacitor and battery pack power split during operation.

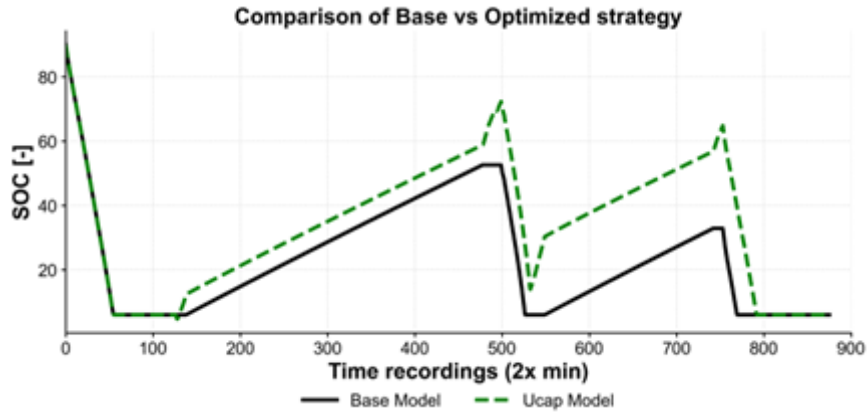


Figure 12 SOC of base model vs SOC of the optimized vessel with the SC and the new EMS.

2.2.4 Ship models (baseline & AENEAS integrations) for use-case 3

2.2.4.1 Baseline ship model

The 3rd case is an inland-shipping vessel that executes cargo transportation trips in the river of Danube. This use-case belongs to the inland domain of the shipping transportation sector, while the previous two belong to short-sea shipping.

- **General characteristics and topology**

Here it is examined a smaller ship than two previous use cases with a different sailing profile typically met on ships that sail in rivers. The ship has also different typological characteristics, subject not only to the utility type of the ship but also related to its powertrain type that is characterized by the absence of any level of hybridization in its design. Figure 13 displays the route that the inland ship follows as well as the speed profile that corresponds to the activity on that route.

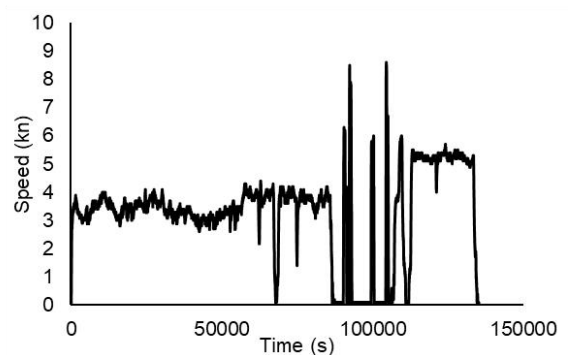
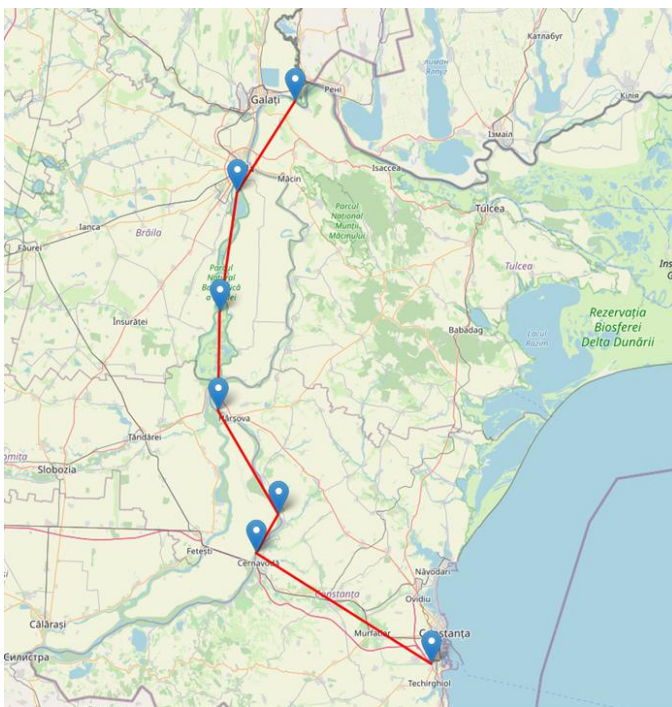


Figure 13. Example route of the Inland shipping ANACONDA vessel route and speed profile

The trip activity on that route is characterized by the following statistics: the cruising phase has an average speed of approximately 7 kn and duration of 30 hours, the stay in ports is of 6 hours total duration, while the maneuvering phase accounts for a duration of less than an hour on average.

The architecture summary of this use-case is provided in the following bullet points:

- Main engines: 2 x 1118 kW
- No Shaft generators
- Bow thrusters: 2 x 399 kW
- Electric generators: 2 x 93 kW

- **Baseline energy management strategy**

This ship baseline strategy is not complex as it is a fully conventional ship not equipped with any type of hybrid energy storage system, nor shaft generators for auxiliaries' coverage. So, the propulsion needs are evidently covered by the MEs and the auxiliary needs by the AEs. An AE also covers the needs of bow thrusters during maneuvers.

- **Model re-parametrization**

The model in Simcenter Amesim was re-parametrized with the actual geometric characteristics of the ship to conduct simulations for the analysis that examines the variation in consumption and emissions under the change of physical parameters. The new parametrization of the ship is provided in the following table.

Table 6 Geometric characteristics necessary for the Holtrop and Mennen method (use case 3).

Ship Parameters	Value	Unit	Source
Nominal Mass	4400	tones	Deliverable D1.1
Length	135	m	Deliverable D1.1
Waterline length	132	m	Deliverable D1.1
Draft	3.17	m	Deliverable D1.1
Breadth	11.4	m	Deliverable D1.1
Transverse bulb area	2	m ²	Assumption*
Center of bulb area	1	m	Assumption*
CB	0.9019	-	Calculated
CP	0.911	-	Calculated
CM	0.99	-	Calculated
CWP	0.9318	-	Calculated

- **Model re-validation**

A revalidation of the model was conducted to obtain as much as possible valid mode outputs. Results of this revalidation are provided in the following figure with good agreement during the cruising phase but some inconsistencies in maneuvering due to lack of data.

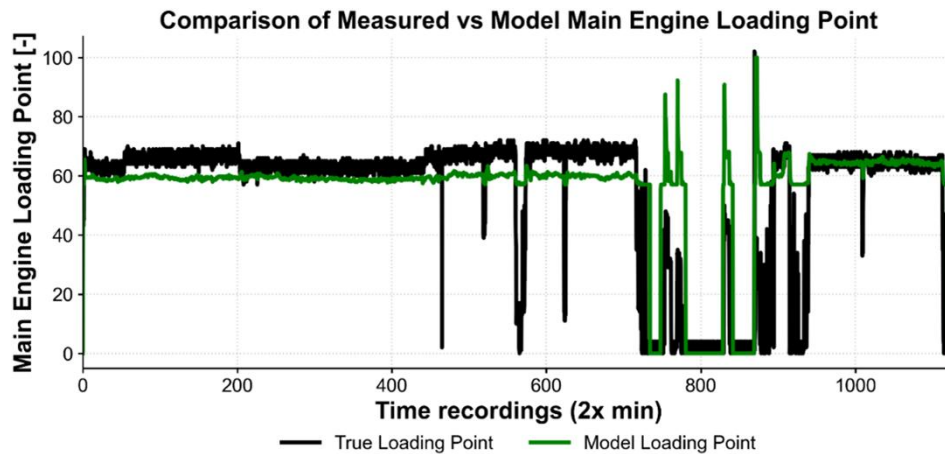


Figure 14 Comparison of main engine loading point, model vs recordings.

2.2.4.2 Ship model after AENEAS solutions integration

- *Ship topology's new characteristics*

In this case, the focus is on the integration in the ship design of a hybrid energy storage system consisted by a SSSB and a supercapacitor. The ship previously didn't have such an electrified system, and so the new design replaces part of the thermal powertrain. In particular, the current diesel generators are swapped with batteries and supercapacitor system. The new characteristics along with the updated layout are provided in the following Table 7 and Figure 15.

Table 7 New vs old ship topology modifications (use case 3).

Parameter	Parameter	Baseline model	Model after AENEAS
Battery	Cell Type	-	Lithium ion
	Cell Capacity [Ah]	-	107
	Number of battery packs	-	1
	Num of cells in series	-	100
	Num of cells in parallel	-	3
	Total Pack energy [kWh]	-	~ 130
	Energy density-gravimetric [Wh/kg]	-	>200
Supercapacitor	Capacity [F]	-	3000
	Min Voltage [V]	-	0
	Max Voltage [V]	-	2.7
	Energy Density [Wh/kg]	-	5.6
	Pack Total Energy [kWh]	-	38 kwh
	Pack Total Power [kW]	-	2 MW

Parameter	Parameter	Baseline model	Model after AENEAS
Energy management strategy	Energy management strategy	-	Hybridization with replacement of diesel generators

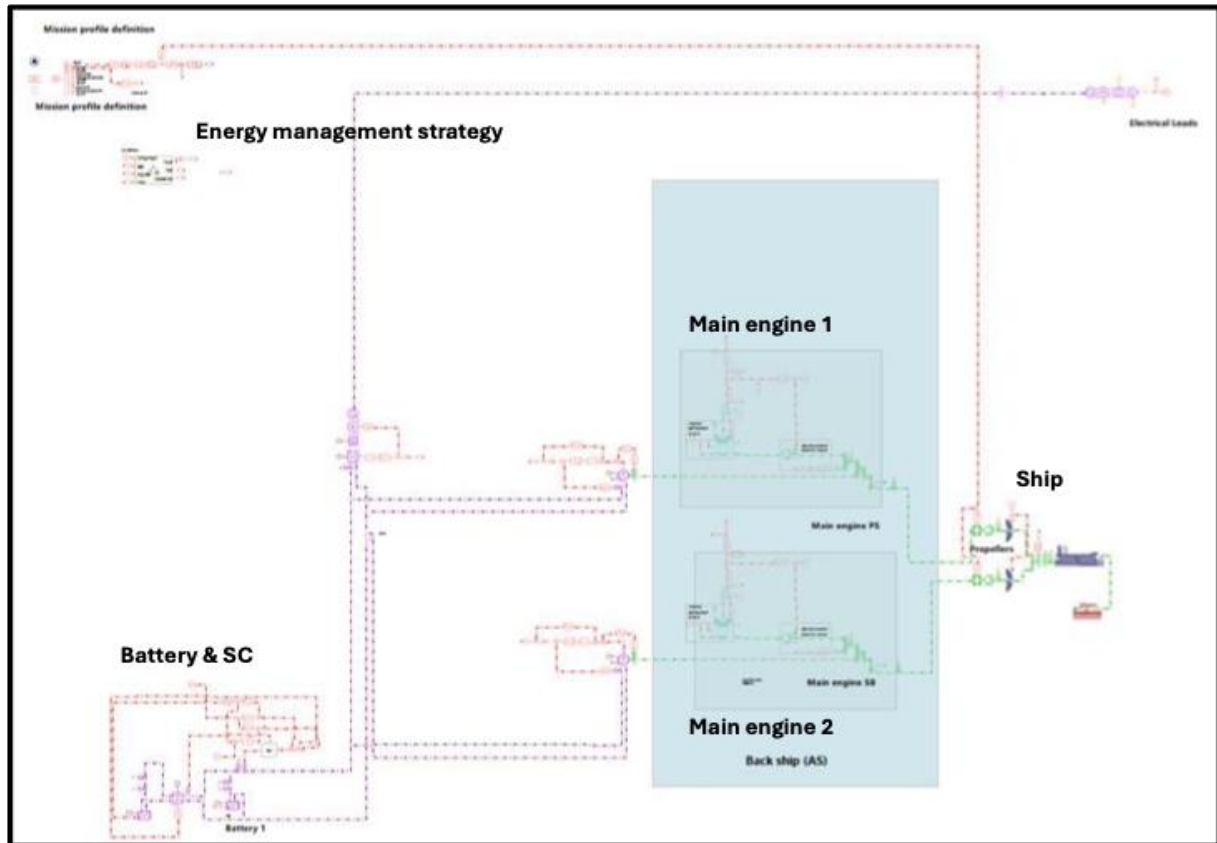


Figure 15 Model in Simcenter Amesim with the updated layout of hybridization

- ***New energy management strategy***

The new energy management strategy of the model as seen in Figure 16, mainly relies on using the battery during port-stay to cover the auxiliary needs. This battery is charged during cruising by the shaft generators that are also integrated into this new design.

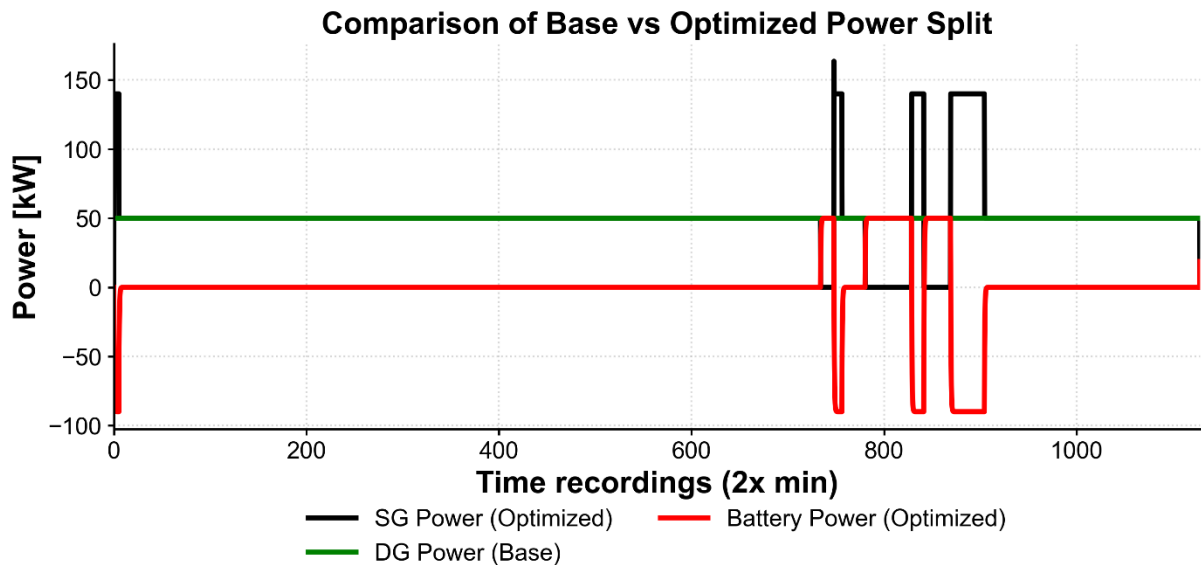


Figure 16 Power split comparison Base vs Optimized architecture for use case 3.

Battery power is positive during the discharge phase and negative during the charge phase.

2.3 Operating situations

2.3.1 Overall parameters examined

This study examines the viability of the new AENEAS designs through parametric analysis, as numerous parameters can influence ships performance during real-world sailing. Many of the parameters vary continuously over time, so their temporal differentiation must be also considered. In addition, these parameters act simultaneously during operation, creating combined—often multiplicative—effects on ship performance.

For these reasons, this deliverable adopts a Monte Carlo simulation as an appropriate method for conducting the required parametric analysis, meeting the requirements for an evaluation of the design viability while accounting for the time-varying nature of multiple influencing parameters acting simultaneously on the ship.

The parameters that are examined are of two broader categories:

- operational (concern external characteristics related to the trip - mainly environmental conditions)
- ship design characteristics (concern internal factors of the powertrain mainly related to technical aspect of the new design)

Environmental conditions data was retrieved from three well-recognized and publicly available databases. Each source provides a different class of environmental parameters relevant to the operation and probabilistic modeling of the vessel. Environmental data were obtained from ERA-5 [5] and Copernicus Marine Service [6], covering wind speed, ocean currents, wave period, and wave height. The raw datasets were downloaded in NetCDF format, converted to CSV via Panoply, and spatially and timed averaged over the operational area of each specific vessel during the whole 2024 year. Statistical distributions (e.g. Normal or Lognormal) were fitted to the resulting space-time series to capture environmental variability.

Ship design parameters (cell capacity, and total ship mass) were modelled using Normal distributions to represent manufacturing variability on the new ESS system and operational uncertainty represented by the loading variation.

Table 8 Parameters used to perform the MC simulation of the optimized architectures

Category	Parameter	Symbol used	Source
Design	Battery Cell / Capacitor Capacity	Qcell / Qcap	Deliverable 1.1
Design / operational	Ship mass loading	mass	Deliverable 1.1
Operational	Wind Speed	wind_speed	ERA 5
	Wind Direction	wind_dir	ERA5
	Current Velocity	Vcp	Copernicus
	Wave Height	H0	Copernicus
	Wave period	Tw0	ERA 5
	Wave direction	wave_dir	ERA 5
	Ambient - Surface -Temperature	surf_temp	ERA 5
	Ambient - Surface - Pressure	surf_press	ERA 5

In total 8 environmental and 2 design parameters were selected as depicted in Table 8. The distributions for each variable under consideration are specified for each use case based on the operating area of the vessel. Distributions for the 8 **environmental parameters** are provided also in Figures 15-17 per use case.

• **Use-case 1 environmental variables distributions**

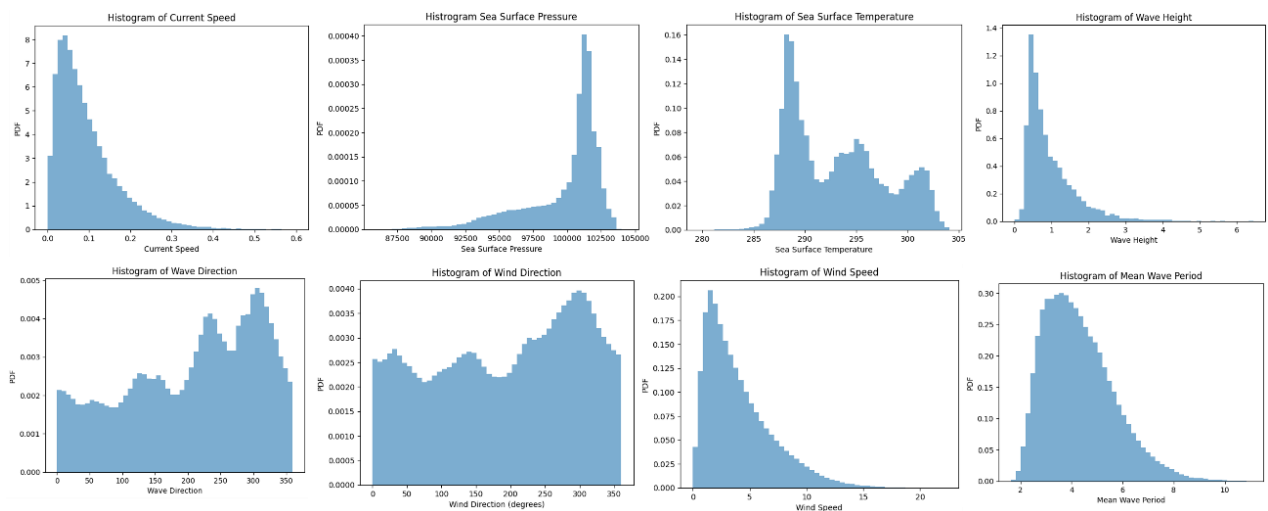


Figure 17 Use case 1 variables distribution.

• **Use-case 2 environmental variables distributions**

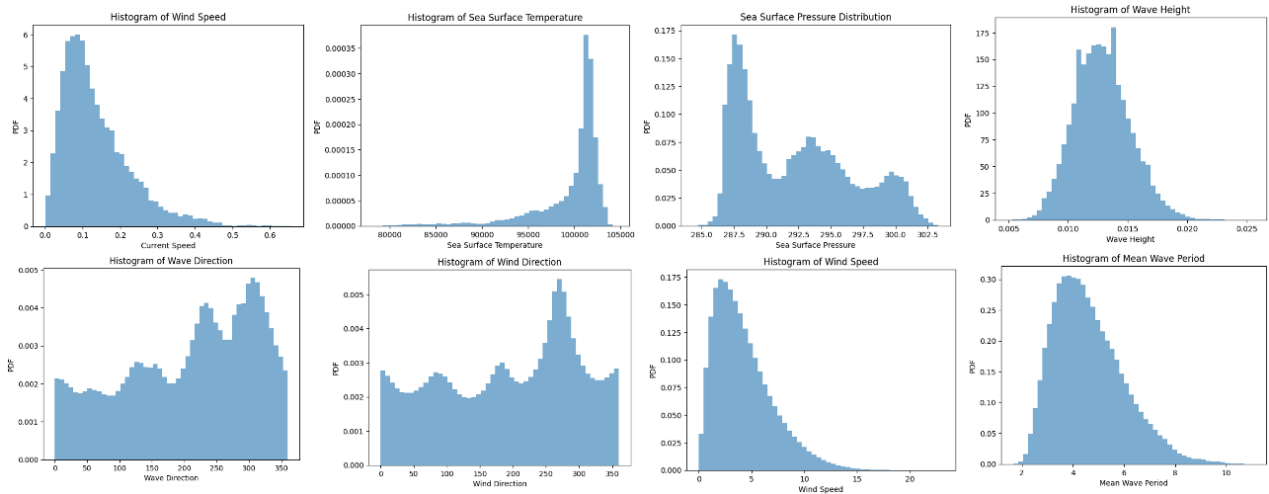


Figure 18 Use case 2 variables distributions.

- **Use-case 3 environmental variables distributions**

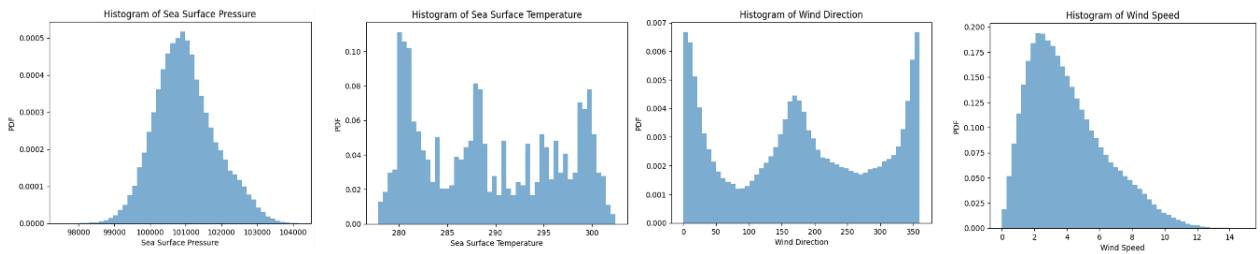


Figure 19 Use case 3 variables distributions.

Not all environmental parameters were varied during each phase of the voyage. For example, during port stays, the vessel speed was fixed to zero, therefore, wind speed, wave height, and current velocity were also set to zero, since varying these parameters would inherently induce vessel motion and thus violate the zero-speed condition.

For **operational parameters**, we modelled both vessel displacement and ESS capacity using normal distributions. For mass loading, we constrained the parameters such that the maximum manufacturer-reported limit remains at least two standard deviations above the mean 95% of the time, ensuring high statistical confidence in operational safety. By adjusting cell capacity (Ah), we evaluate the total energy available during port stays, a variation achievable in the real ESS system through either physical system scaling or the optimization of State of Charge (SOC) windows. To maintain consistency across all use cases, we applied a uniform Coefficient of Variation (CV) for capacity and displacement distributions respectively.

All the parameters (**environmental and operational**) affect directly or indirectly many additional parameters. For example, the ship mass alters the ship geometrical hydrodynamic coefficients, wave height and current speed, affect directly the propeller efficiency and the power output of the main diesel engines.

2.4 Simulations with Monte Carlo

2.4.1 Monte Carlo Method overview description

The Monte Carlo simulation methodology was employed to assess the robustness and viability of the optimized vessel design under realistic operational uncertainties. This probabilistic approach allows key model input parameters (e.g., component efficiencies, environmental conditions, mission loads) to be represented not as fixed values but as probability distributions, thereby reflecting the inherent randomness of real-world conditions. Instead of providing a single deterministic output, the method generates a range of possible outcomes, quantifying both their likelihood and variability. This enables a deeper understanding of the system’s behaviour across hundreds of virtual realizations that would be not possible with single run simulations.

By repeatedly sampling parameter combinations and running the Digital Twin model for each case, the Monte Carlo methodology produces statistical distributions of the selected target variables such as fuel consumption, power demand, and emissions. These results enable the estimation of confidence intervals, identification of worst- and best-case scenarios, and evaluation of design robustness i.e., whether the optimized system maintains acceptable performance despite parameter uncertainties. Furthermore, sensitivity analysis performed on the Monte Carlo dataset highlights the most influential parameters driving performance variation, supporting informed design decisions and risk quantification. Overall, this methodology provides a probabilistic verification of the optimized design, ensuring that it remains viable and reliable across a realistic range of operating conditions.

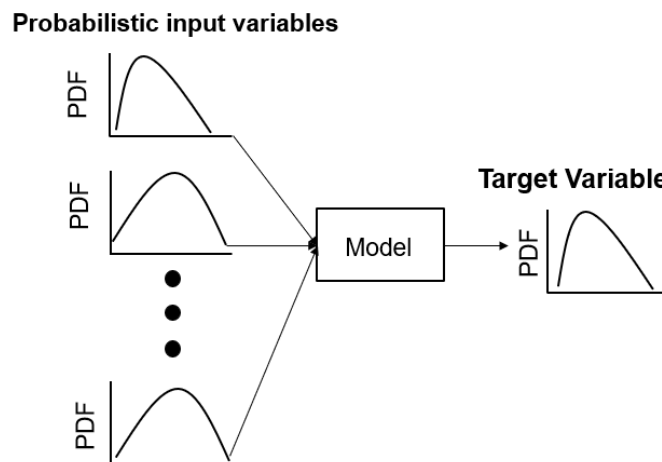


Figure 20 Schematic of Monte Carlo Methodology

The Monte Carlo methodology applied for the verification of the optimized vessel design follows a structured workflow that ensures statistical soundness of all computational steps. The process can be divided into five main stages described in the following section.

2.4.1.1 MATLAB-Simcenter Amesim connection and Model Execution

Figure 21 illustrates the Monte Carlo–based robustness analysis workflow developed to evaluate the vessel’s performance under uncertainty. The process begins with the definition of key environmental and ship design input parameters and the assignment of appropriate probability distributions to each variable, based on experimental data or expert assumptions.

1. Parameters and their Distributions:

Each uncertain parameter is modelled as a random variable following a defined distribution (e.g., normal, uniform, log-normal). These serve as the input uncertainty sources.

2. Monte Carlo Sampling (MATLAB):

A MATLAB script executes the Monte Carlo sampling routine, generating hundreds of random parameter combinations using built-in sampling methods (such as the Latin Hypercube Sampling). MATLAB automates the random draw process and stores each sampled parameter set for simulation. This forms the complete parametric space to be tested, serving as the foundation for the subsequent automated simulations in Simcenter Amesim.

3. Simcenter Amesim Model Execution:

For each sampled set, MATLAB communicates directly with the Simcenter Amesim Ship Model via scripting interfaces. Using this built in Amesim functions, MATLAB dynamically updates Amesim model parameters continuously, triggers simulations, and retrieves output data programmatically, eliminating the need for manual intervention.

4. Output Variable Distribution:

After all simulations are completed, MATLAB post-processes the results, aggregating the outputs (such as fuel consumption, total CO₂ emissions, etc.) into statistical distributions. This allows computation of mean, standard deviation, confidence intervals, and sensitivity indicators across all generated scenarios.

In summary, MATLAB acts as the Monte Carlo controller, data manager and post processor, while Amesim functions as the high-fidelity physics model. Their interaction is fully automated through script-based parameter injection, model execution, and result extraction, forming a seamless MATLAB-AMESIM co-simulation loop for fast and accurate probabilistic digital twin validation.

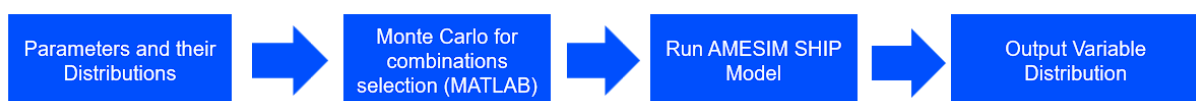


Figure 21 MATLAB-Amesim scripted based communication

2.4.1.2 Sampling and Required Sample-Size Selection

- **Latin Hypercube Sampling (LHS)**

To explore the uncertainty space of the vessel's Digital Twin model, **Latin Hypercube Sampling (LHS)** was employed as the parameter sampling technique. LHS is an advanced sampling method that improves the statistical representativeness of the input space compared to simple random sampling, especially when dealing with a large number of uncertain parameters.

In the LHS approach, the range of each input parameter's probability distribution is divided into N equally probable intervals. From each interval, one random value is selected, ensuring that all portions of the distribution are represented exactly once. These selected values are then

randomly paired across parameters to form N unique parameter sets (samples). This process guarantees that the full range of each variable is systematically covered without requiring an excessively large number of simulations as seen in Figure 22, [7].

In the context of this task, LHS was used to generate a diverse and statistically balanced set of input combinations for the Monte Carlo analysis. This ensured that the Digital Twin simulations explored the full operational uncertainty space efficiently, enabling reliable estimation of system robustness and performance variability.

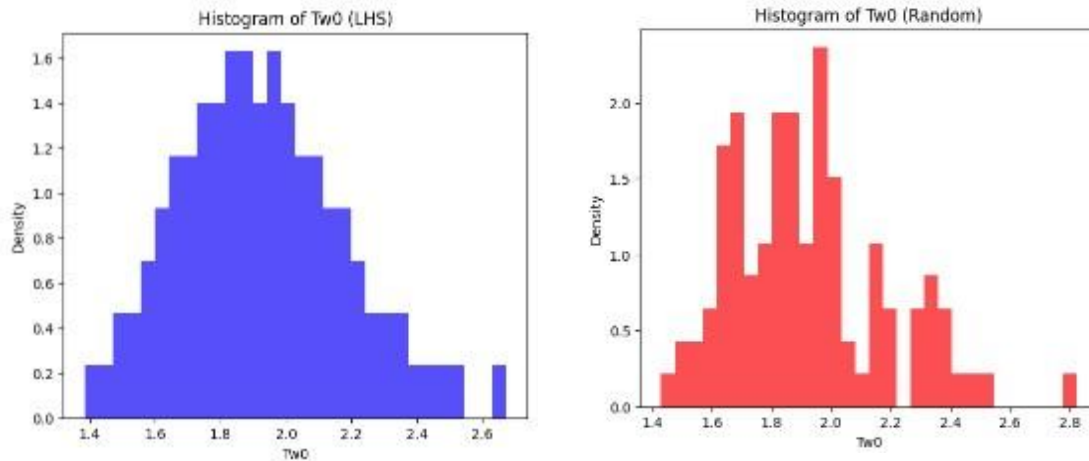


Figure 22 Latin Hypercube coverage of the parametric space vs random sampling for 50 total samples for a random variable.

- **Required sample size selection**

The formula for the critical sample size N is derived from the maximum absolute error of the sample mean when estimating the population mean, based on the central limit theorem [8].

$$N_{critical} = \left(\frac{Z_{\alpha/2} \sigma_{xi}}{Ere \mu_{xi}} \right)^2 \quad (17)$$

To minimize computational cost, the total number of Monte Carlo simulations was capped at 500. The final simulation count is therefore determined as:

$$N_{final} = \min (N_{critical}, 500)$$

where $N_{critical}$ is the statistically required sample size calculated from the convergence criterion above.

Upon completion of each Monte Carlo run, a Kolmogorov-Smirnov (K-S) test is performed to verify that the 500 samples per variable adequately represent their respective population distributions. This ensures statistical validity of the simulation results despite the imposed cap.

2.4.1.3 Statistical Consistency Check (Kolmogorov–Smirnov Test)

To ensure that the generated random samples faithfully represent the theoretical probability distributions that are derived from, the one-sample Kolmogorov–Smirnov (K–S) goodness-of-fit test was applied. The test compares the empirical cumulative distribution of the sampled data with the theoretical CDF and quantifies their maximum deviation. If the K–S statistic lies below the critical value at a chosen confidence level α , the sampling is considered statistically consistent.

Empirical distribution function

The empirical distribution function at the value x represents the proportion of data points that are less than or equal to x in the sample. Given a set of n samples x_1, x_2, \dots, x_n , the empirical cumulative distribution function - CDF is defined as:

$$F_n(x) = \frac{1}{n} \sum_{i=1}^n 1_{\{x_i \leq x\}}, \quad (18)$$

For a given significance level, α , the K-S statistics are calculated as:

$$D_n = \sup_x |F_n(x) - F(x)| \quad (19)$$

were:

- \sup stands for supremum, which means the largest value over all possible values of x .
- $F(x)$ is the theoretical cumulative distribution function (e.g., normal, exponential).
- $F_n(x)$ is the empirical cumulative distribution function of the sample (calculated as described above).

Hypotheses Formulation

- **Null Hypothesis H_0 :** The sample follows a specified distribution.
- **Alternative Hypothesis H_1 :** The sample does not follow the specified distribution.

Critical Value

The $D_{n,\alpha}$ is the critical threshold corresponding to:

- The sample size n
- The significance level α (e.g., 0.05 or 0.01).

In most cases the values for the critical threshold are calculated directly from K-S tables using the following approximation formula:

$$D_{n,\alpha} = \frac{c(\alpha)}{\sqrt{n}} \quad (20)$$

Where constants such as $c(0.05) = 1.36$ and $c(0.01) = 1.63$ depending on the significance level α value.

We fail to reject the H_0 and conclude that the sample data is statistically consistent with the target distribution if and only if:

$$D_n < D_{n,\alpha} \quad (21)$$

We reject H_0 and conclude that the data likely do not come from that distribution if:

$$D_n \geq D_{n,\alpha} \quad (22)$$

2.4.1.4 Post-Processing and Result Analysis

Once the Monte-Carlo simulations were completed and the generated samples passed the statistical checks, the next step was to interpret what the results mean for the system. Post-processing focuses on turning large amounts of raw simulation data into clear, understandable

insights: how the output behaves, how sensitive it is to each uncertain parameter, and which factors matter the most.

- **Target variable distribution identification**

Distribution characterization of the target variable: mean, median, variance, and skewness of each target variable were computed, and the type of resulting probability distribution was identified. Multiple candidate probability distributions (e.g., normal, log-normal, gamma, t - location scale) were fitted to the data, and model quality was assessed using the Akaike Information Criterion (AIC). The distribution with the lowest AIC was selected as the best representation of the underlying data-generating process.

- **Correlation analysis (Spearman)**

The Spearman correlation coefficient was used to quantify the linear or monotonic relationships between each input parameter and the output target variable.

It operates on the ranked values of variables:

1. Convert x_i and y_i to ranks $R(x_i)$ and $R(y_i)$
2. Compute the Pearson's formula on the ranked pairs

The resulting formula for the Spearman rank correlation coefficient ρ_s is the following:

$$\rho_s = \frac{\sum_{i=1}^n (R_i - \bar{R})(S_i - \bar{S})}{\sqrt{\sum_{i=1}^n (R_i - \bar{R})^2} \sqrt{\sum_{i=1}^n (S_i - \bar{S})^2}} \quad (23)$$

Because Spearman uses ranks, it is robust to nonlinearities and outliers, making it especially valuable when the response varies smoothly but not necessarily linearly with an input parameter.

Correlation 1 means that the two variables move with identical relative displacement. When one variable changes by one unit in its own scale (1 standard deviation from its mean), the other variable also changes by one unit in its own scale (1 standard deviation from its mean).

- **Multilinear regression analysis**

A regression model was fitted to determine the relative influence (sensitivity) of each uncertain parameter on the target variable, thereby ranking their importance. The target variable is expressed as a linear combination of several input variables, allowing the estimation of each parameter partial contribution while holding all the rest constant.

For a target variable Y and predictors X_1, X_2, \dots, X_n , the regression model is:

$$Y = \beta_0 + \beta_1 X_1 + \beta_2 X_2 + \dots + \beta_n X_n + \varepsilon \quad (24)$$

However, a notable limitation is the method's reliance on linearity. The model assumes that the effect of each input on the output is linear and additive. If the true relationship is strongly nonlinear or involves interactions between parameters, multilinear regression may misrepresent and over-underestimate the underlying sensitivity.

To identify the most informative predictors for the regression model, all candidate variables were first ranked according to their Mutual Information (MI) with the target (cumulative emissions). MI captures any type of dependency, linear or nonlinear, making it a more general relevance metric than simple correlations. The MI indicates how much information can be obtained from a random variable by observing another random variable. It is the reduction of

uncertainty of a variable if another one is known. High MI indicates large reduction in uncertainty while low value small. If MI is zero, the two variables are independent.

For two random variables it is defined as:

$$MI = \sum_x \sum_y p(x, y) \log \left(\frac{p(x, y)}{p(x)p(y)} \right) \quad (25)$$

Where $p(x, y)$ is the joint probability and p is the marginal probability for x and y respectively.

The variables were then sorted by MI in descending order, and models were fitted using the top-N predictors. For each N, a pure multi-linear model was trained, and its performance was evaluated using the RMSE metric. The final number of predictors was selected at the point where RMSE value was minimized.

- **Robustness and risk metrics**

Confidence intervals, probability of exceeding performance thresholds, and worst/best-case scenarios were extracted to quantify the system's reliability under uncertainty.

3 Results for use-case 1

This section presents the results of the Monte Carlo simulation, for both the baseline and the optimized electrified architecture. The target variable of the simulation is the cumulative emissions of CO₂ produced by the vessel in each operating condition along the selected trip: cruising, acceleration, deceleration and port stay. By repeatedly running the simulation with varying environmental and ship design parameters we can quantify how total emissions fluctuate under realistic-probabilistic operating conditions. The primary objective of the electrified architecture is to reduce emissions in and around the port area during arrival and departure.

The following results show how effectively the optimized system achieves this goal across the relevant operating modes. In addition, the sensitivity analysis is carried out to quantify how each input parameter influences the target variable.

It is noted that expected fuel consumption reduction is similar to CO₂ because of their proportional relationship.

3.1 Cumulative CO₂ Emissions Results

3.1.1 Cumulative Emissions comparison

First, we select to present CO₂ results outside of the MC simulation. This step was conducted to take account one parameter in addition to the environmental and the design-related ones, which is variability in the trip characteristics (trip phases duration, speed profile dynamics). So, in this part we consider more than one trip on the same route in the simulation without changing any other of the examined parameters. Reasons of increased computational time of MC implied this choice to disengage this parameter.

The overall trip results, for a total of 209 hours of recorded data, are provided in the table below where the absolute values in terms of CO₂ emissions are depicted for entire trips, as well as per trip mode along with the percentage difference achieved after AENEAS.

Table 9 Comparison of cumulative CO₂ emissions over the full duration for a single run (use case 1).

	Total	Cruising	Acceleration	Deceleration	In-port
Baseline (tn CO₂)	930.1	836.5	24.65	26.84	42.13
Optimized (tn CO₂)	924.6	841.1	22.23	21.85	39.38
% Difference	-0.6	0.54	-10.6	-22.84	-6.97

Looking at the overall trip picture, total fuel consumption/CO₂ emissions are slightly reduced verifying the effectiveness of the hybridization strategy of AENEAS that operates the bigger and more efficient engines to produce electricity and relief the less efficient auxiliary engines. Effects despite being minimal show that there isn't any additional fuel cost to achieve zero-pollutant emission port operations, even ME operate at a higher load to charge the batteries. It is noted that these benefits are additional ones to the initial level of hybridization that already exhibited some benefits to this ship compared to a similar one that was not hybrid at all. These results also indicate that semi-solid-state battery technology does not negatively affect the performance of the ship, a strong indication of the viability of the new design.

Monte Carlo Simulation Results

For the MC simulation purposes that evaluates the operational and design parameters, a smaller part of recordings was used (61.5 hours), that however covered a complete trip from Genova to Catania and a total of 3 port stays, including the intermediate stop at Livorno. The comparative results are represented below:

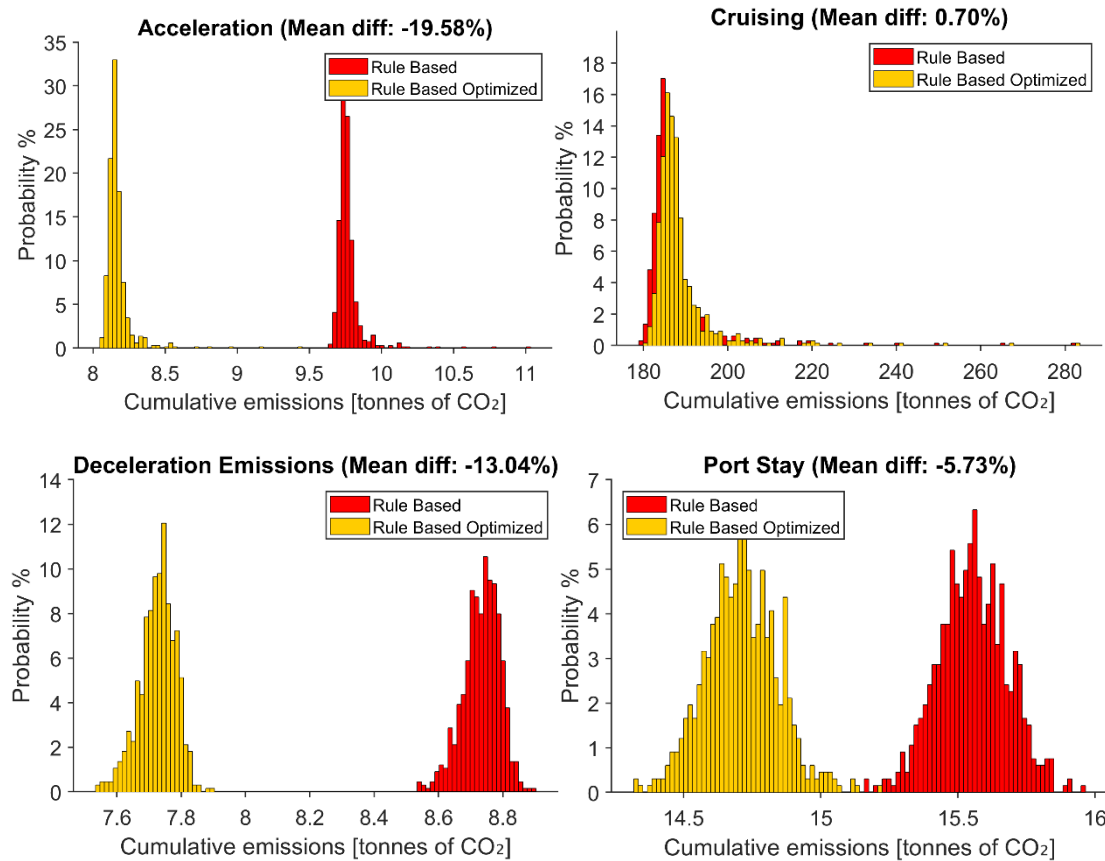


Figure 23 Probability distribution comparison for different trip phases between base and optimized vessel architecture (Use case 1).

The emission distributions produced by MC in varying operational and design parameters also verify the gains previously seen in multiple trips. This is visualized in Figure 23 as well as in Table 10, for the entire trip and per trip mode.

Additionally, both strategies produce results that appear to follow the same underlying distribution type for every trip phase. The primary difference is a horizontal shift in mean/median, not a change in shape, spread, or tail behavior. Relative uncertainty is preserved and that makes the systems relatively stochastic behavior the same across both architectures. The MC simulation has proven that optimization does not introduce new sensitivities that would amplify input uncertainties into extreme emissions spikes. Electrified architecture maintains a level of robustness comparable to the base case, exhibiting no significant reduction in performance variance or sensitivity to uncertainty.

Table 10 Aggregated results for the mean value difference of CO2 emissions for the specific MC trip (use case 1).

	Total	Cruising	Acceleration	Deceleration	In-port
Baseline (tn CO2)	221.42	187.37	9.77	8.73	15.55
Optimized (tn CO2)	219.30	188.69	8.17	7.73	14.71
Difference	-0.97	0.7%	-19.58%	-13.04%	-5.73%

Acceleration

The acceleration phase exhibits the most noticeable improvement in the reduction of CO₂ emissions. This is extremely important since this emission is close to the shore. The optimized architecture shifts the whole distribution towards lower emissions with a mean reduction of about ~ 20 %. The optimized strategy operates with only auxiliary engine running at the higher load but at a better efficiency point. Additionally, the strategy prevents battery charging during acceleration, ensuring that the propulsion and electrical energy demands are met without any additional load spikes on the auxiliary engines. These operational choices have a direct influence on the shape and position of the emission distributions observed in the Monte Carlo analysis.

Deceleration

Deceleration shows also similar improvement. The optimized configuration results in a mean reduction of roughly -13%.

Cruising

In cruising, the optimized strategy results in a slight increase in emissions. The probability distribution for the optimized case shows a slight shift to the right, corresponding to a ~0,7 % increase in mean cumulative emissions. In both the baseline and the optimized architecture, the battery is recharged through the shaft generator. The difference lies in the charging rate and the associated losses, which depend on the specific ESS configuration. The optimized system charges at a higher rate and experiences additional conversion losses compared with the baseline setup. These factors increase the mechanical load on the main engine, which explains why optimized architecture results in slightly higher cruising emissions.

Port Stay

Port stay exhibits a meaningful reduction of mean total emissions, driven by auxiliary engine efficiency and higher available ESS system energy. This behavior arises because the optimized strategy prioritizes maximizing hotel energy availability by avoiding battery usage during maneuvering phase. Additionally, with hotel loads dominating this phase, the optimized strategy running a single auxiliary at higher, more efficient load produces a clearer left shift in the emission distribution and a ~ 6 % decrease in mean emissions. The variability of both the optimized and base scenarios is associated directly with the variability of the ESS system's total available energy which is directly affected by the capacity of the batteries measured in Ah. This variable is the only parameter varied in the simulation during the port stay phase. Since ESS capacity reflects both design-phase sizing decisions and capacity degradation over lifetime, the observed emission variability can be interpreted as a sensitivity to these two factors.

3.1.2 Target variable distribution identification and characterization

Next step it to fit a theoretical distribution to the Monte Carlo results, to transform the discrete simulation data into a continuous mathematical model, providing a clearer analytical framework for assessing risk and system reliability. The distribution characteristics of the target variable for every trip phase for the optimized architecture is presented in the following table:

Table 11 Results for the best fitted distribution for each trip phase for the optimized architecture (use case1).

Trip Phase	Distribution Type	Mean	Std
Acceleration	t-Locationscaled	8.17	0.01

Trip Phase	Distribution Type	Mean	Std
Deceleration	Normal	7.73	0.056
Port Stay	Normal	14.71	0.13
Cruising	t-Locationscaled	188.7	8.178

When the distribution of a given set of data has heavier tails (more prone to outliers) than the normal distribution, a t location-scale distribution can be exploited. In addition to the mean, and standard deviation, the t location-scale has an additional shape parameter, ν , to capture the heavier tails. Thus, a t location-scale distribution can be fully characterized if the values of μ , σ , and ν are known.

Fitting results between fitted distribution and simulation results are presented in the graph below:

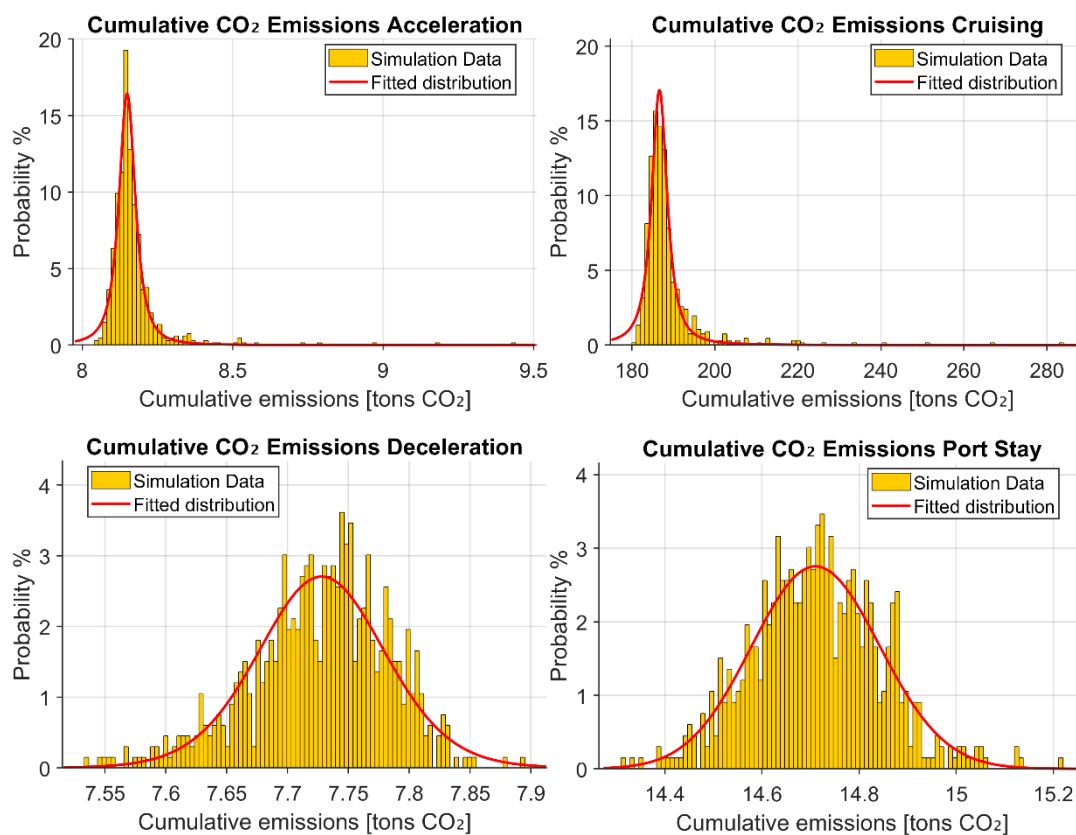


Figure 24 Fitted distributions for each trip phase (Use case 1).

The lognormal distribution gives some rare extreme values that may occur during the crushing or acceleration phase depending on the conditions of the trip.

To quantify the variability in cumulative CO₂ emissions, we extracted key distribution quantiles from the best-fitting probabilistic model. The 5th percentile represents a conservative best-case scenario, the 50th percentile corresponds to the typical (median) expected performance, and the 95th percentile reflects a worse-case upper bound under normal operating uncertainty. These quantile values provide a direct, model-based characterization of the system's expected, optimistic, and pessimistic outcomes, enabling clear comparison of reliability and risk. Table 12 summarizes the estimated emission levels at each quantile and also the minimum and maximum observed values.

Table 12 Percentile Distribution of Vessel Trip Phase Emissions (use case 1).

Trip Phase	5th	50th	95th
Acceleration	8.35	8.44	8.52
Deceleration	7.65	7.73	7.82
Port Stay	14.68	14.89	15.11
Cruising	179.3	186.65	193.98

Based on the percentiles the following are true:

5th percentile

- Only 5% of all possible outcomes are expected to be below this value.
- This is effectively a best-case optimistic scenario.

50th percentile

- This is the median, meaning half of the outcomes are below and half above.
- This represents the typical or central behavior of the system.

95th percentile

- 95% of all outcomes are below this value.
- Only 5% of runs exceed this level.
- This represents a worst case but still realistic scenario.

3.1.3 Hypotheses Analysis on input variables

The results of the one sample K-S test are represented here. The K-S test was used to examine if the drawn sample for each input parameter is representative of the population. If the sampled distributions were not consistent with their populations, the simulation could produce biased/incorrect results. The p – values for all the input parameters are presented in the following table:

Table 13 K-S test results (use case 1).

Parameter	K-S result (p-value)	Interpretation
Battery Cell Capacity	1	Sample is consistent
Wind Speed	1	Sample is consistent
Wind Direction	1	Sample is consistent
Current Velocity	1	Sample is consistent
Wave Height	1	Sample is consistent
Wave period	1	Sample is consistent
Wave direction	1	Sample is consistent
Ambient Temperature	1	Sample is consistent
Ambient Pressure	1	Sample is consistent
Ship mass loading	1	Sample is consistent

Since the p-value for all parameters is 1 we fail to reject the H0 hypothesis and we can safely conclude that all samples are representative of their respective population distribution.

The resulting distribution of some selected variables are represented in the following figure in comparison to the theoretical distribution derived from the environmental data.

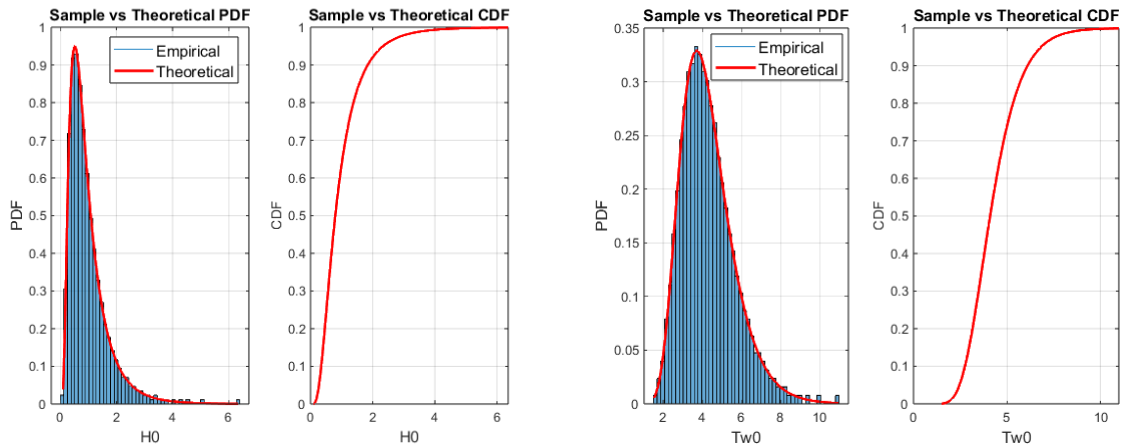


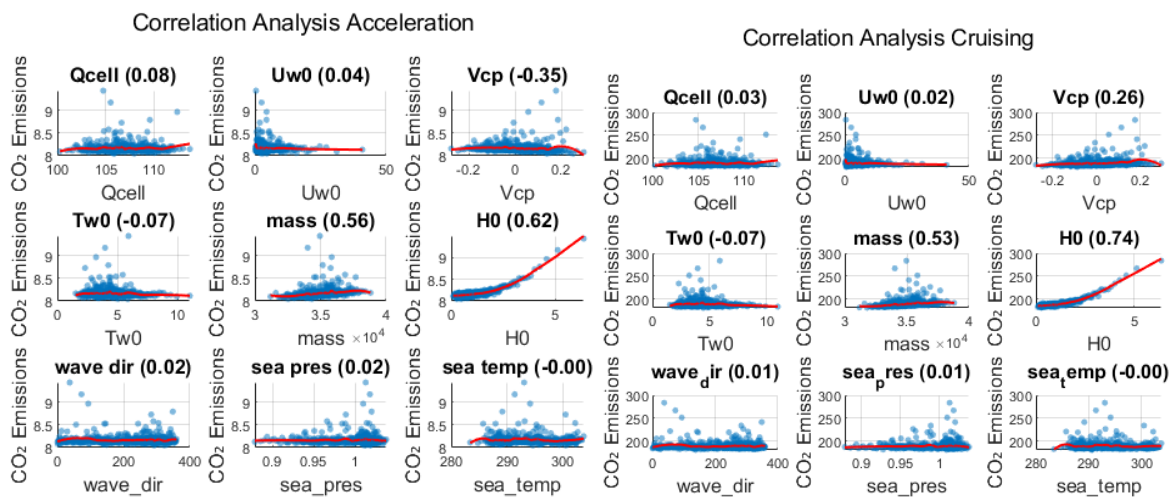
Figure 25 K-S results for wave height and wave period (Use case 1).

The success of the K–S test here is expected, as the Latin Hypercube Sampling strategy produces samples that efficiently cover the full range of each variable, yielding distributions that are highly representative of the theoretical distributions that characterize the populations of these variables.

3.2 Sensitivity Analysis on Input Variables

Correlation analysis helps us identify features that are relatively more strongly associated with the total emissions per trip phase, informing feature selection and model design, but it does not quantify their absolute impact on the target variable.

Spearman correlation provides normalized values ($\rho_s \in [-1, +1]$) that are directly interpretable: variables with $|\rho_s| > 0.7$ indicate strong influence to total emissions, while the sign reveals whether increasing the input increases or decreases emissions.



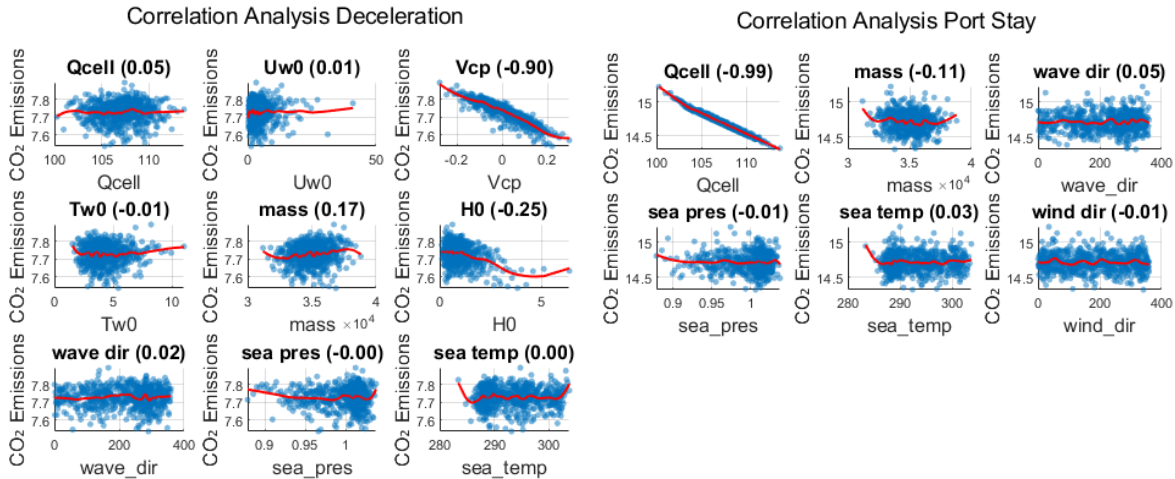


Figure 26 Spearman correlation coefficients for input variables (Use case 1).

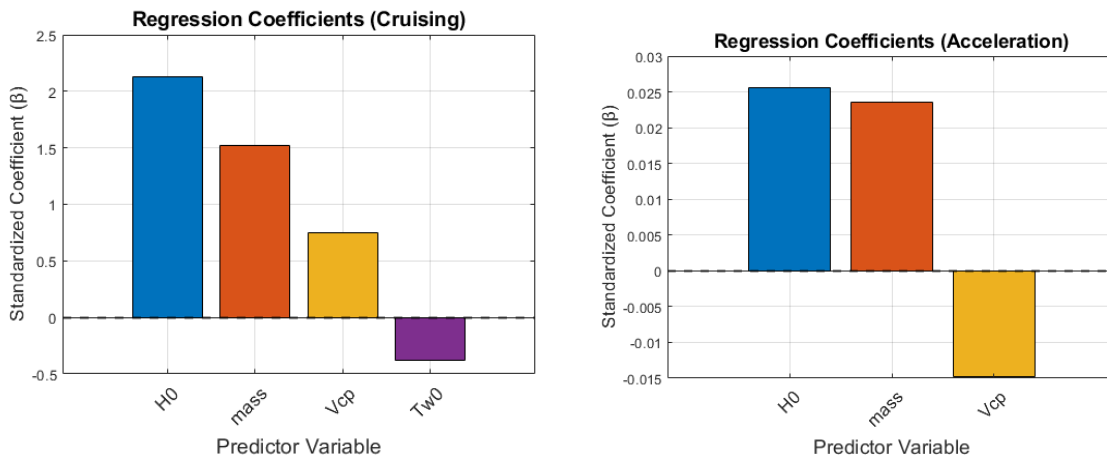
It is evident from Figure 26, that when all the variables are varied simultaneously, the ones that have a direct influence on the total CO₂ emissions are the current speed (Vcp), wave height (H0) and the capacity of the battery (Qcell) which affects the available energy during the port stay.

Spearman correlation can capture monotonic, non – linear relationships but can't capture the absolute magnitude of change that one variable can have on emissions. For this reason, a multilinear regression model was fitted to examine this effect and give a direct and interpretable estimate of the total emissions at every trip phase.

3.3 Reduced surrogate models

The multilinear regression model was fitted to explain and predict cumulative CO₂ emissions using the most informative input variables for every trip phase, meaning we used the top ranked variables based on the Mutual Information towards the target variable.

A summary of the selected predictors, their standardized coefficients, is provided in Figure 27.



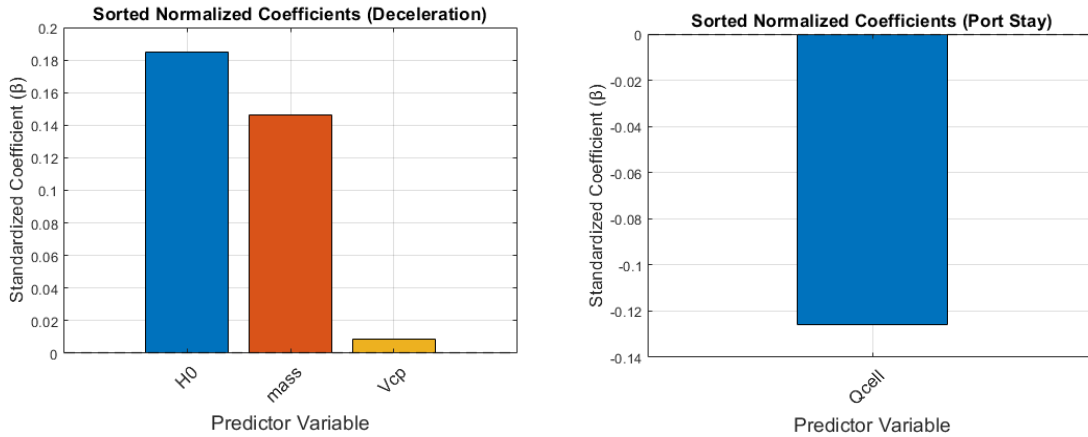


Figure 27 Multilinear regression analysis standardized coefficients (Use case 1).

All features are scaled to mean=0, STD=1 (Standard Deviation). This way coefficients represent: "Change in CO₂ (in standard deviations) per 1 STD change in predictor"

The standardized coefficients quantify each predictor's marginal effect on total CO₂ emissions. This means that positive coefficients indicate increased emissions with higher feature values, while negative coefficients indicate reduction. For each trip phase we can rank the variables directly by importance. Ship loading and wave height are the most important variables affecting the total CO₂ emissions. Fitted Model performance is presented in Figure 28:

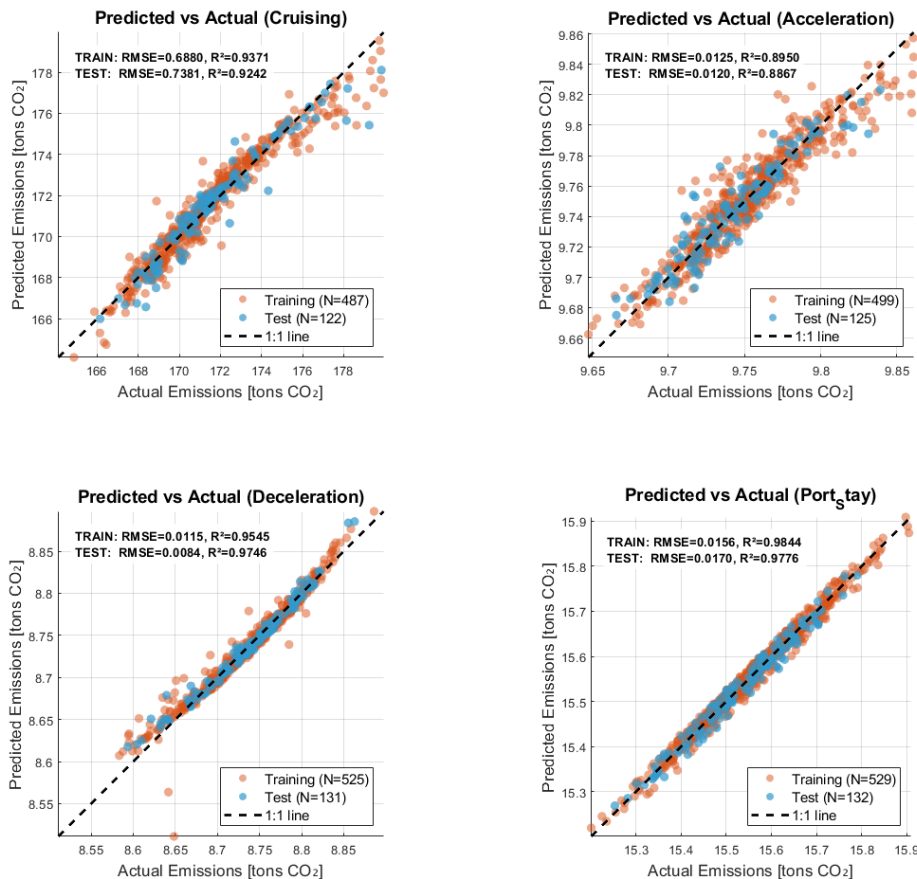


Figure 28 Predicted vs Actual Values for CO₂ emissions. Performance characterization of the multilinear regression analysis (Use case 1).

Deliverable D2.4

The linear model achieves high predictive accuracy for CO₂ emissions, with comparable performance on both training and test sets, indicating good generalization.

4 Results for use case 2

4.1 Cumulative CO₂ Emissions Results

4.1.1 Cumulative Emissions distribution comparison

Results for use case 2 on the single run simulation that evaluates the trip characteristics are provided in Table 14 for a total duration of 142 hours based on the available recordings. In this, the absolute values in terms of CO₂ are depicted for the entire trips as well as per trip mode along with the percentage difference achieved after AENEAS. It is reminded that this evaluation was conducted to take account the variability in the duration of the trip phases, considering more than one trip on the same route.

Table 14 Comparison of cumulative CO₂ emissions over the full duration for a single run (use case 2).

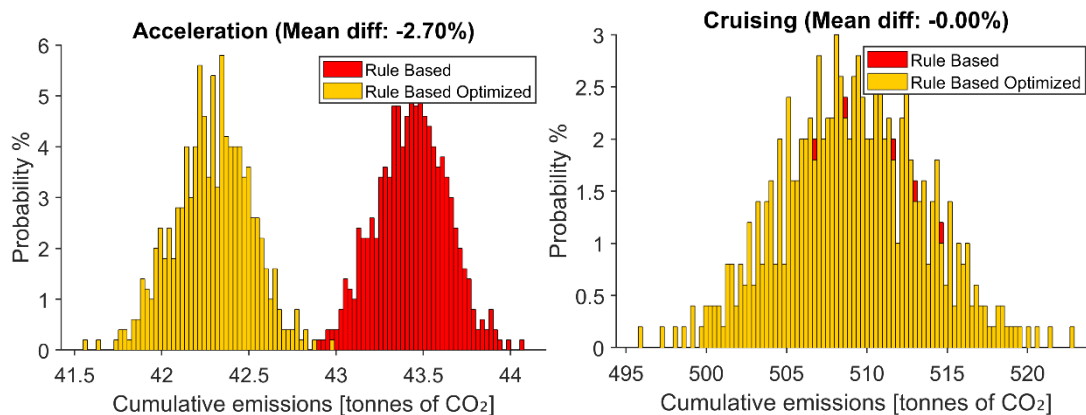
	Total	Cruising	Acceleration	Deceleration	In-port
Baseline (tn CO₂)	2467.1	2212.84	116.1	96.71	41.4
Optimized (tn CO₂)	2417.2	2212.83	109.77	63.76	30.83
% Difference	-2.1	0	-5.75	-51.68	-34.3

Similar to use case 1 the viability of the new design is verified. The integration of a SC in the ship hybrid architecture, together with an optimization of the energy management strategy, provides benefits quantified at 2% in total. Higher gains are observed close to port and during port stay ensuring periods of zero emission port operation. It is noted that these gains also come in addition to the existing ones achieved through the initial hybridization of the ship

Monte Carlo Simulation Results

For the MC simulation purposes, a smaller part of recordings was used, that covered the whole trip from Barcelona to Civitavecchia and a total of 3 port stays, including the intermediate stop at Porto Torres.

The comparative results are represented below under the evaluation perspective where operational and design parameters change:



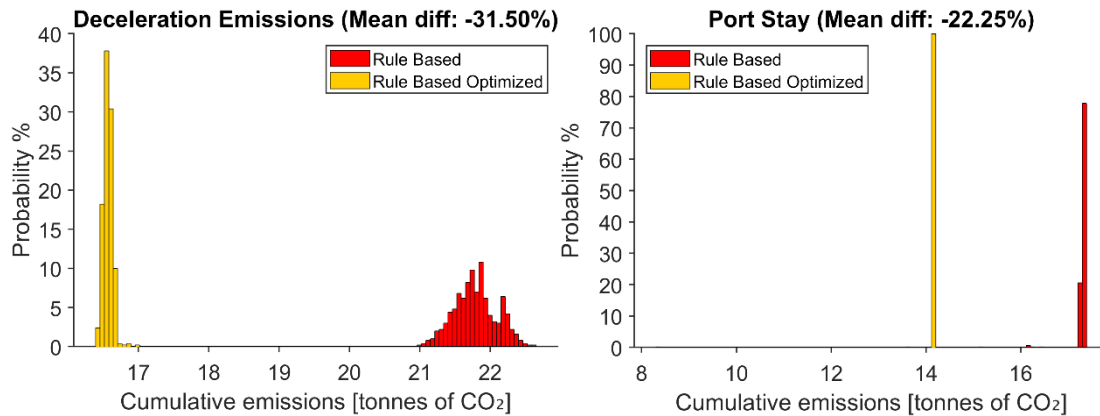


Figure 29 Probability distribution comparison for different trip phases between base and optimized vessel architecture (Use case 2).

The shape of the distributions indicates the following: acceleration phase achieves a minimal reduction of CO₂ emissions, with the same underlying relative system stochastic behavior, while no improvement can be achieved during the cruising phase. Deceleration is the only phase where optimization achieves both mean reduction and variance reduction (CV). Emissions are more predictable across different operating conditions. The system is both cleaner and more consistent/robust. Port stay results are quite deterministic, and the improvement is directly proportional to the higher available energy of the ESS system.

The overall results quantified by the MC are provided in Table 15, verifying the viability of the new design under operational and design parameters that can change during real world operations. An analysis per trip mode follows this table.

Table 15 Aggregated results for the mean value difference of CO₂ emissions for the specific MC trip (use case 2).

	Total	Cruising	Acceleration	Deceleration	In-port
Baseline (tn CO₂)	591.6	509.1	43.43	21.79	17.3
Optimized (tn CO₂)	582.1	509.09	42.29	16.57	14.1
Difference	-1.63 %	0 %	-2.7 %	-31.5 %	-22.25 %

Acceleration

The acceleration phase exhibits an improvement of around ~3%. The optimized architecture focuses on improving engine load and thus efficiency during the maneuvering phase, by enabling the usage of the SC modules as explained in the energy management strategy of this use case.

Deceleration

The deceleration phase exhibits the most noticeable improvement in the reduction of CO₂ emissions for use case 2. Again, this is extremely important since this emission is close to the shore. The mean reduction is about ~ 32 %.

Cruising

In cruising, the optimized strategy results in no significant improvement in total CO₂ emissions.

Port Stay

Port stay emissions reduction of 22% is directly related to the higher battery pack capacity availability. The battery pack is being charged during the navigation phase, plus an additional rapid charge during the maneuvering phase through the SC modules.

4.1.2 Target variable distribution identification and characterization

The distribution characteristics of the target variable for every trip phase for the optimized architecture is presented in the following table:

Table 16 Results for the best fit distribution for each trip phase for the optimized architecture (use case 2).

Trip Phase	Distribution Type	Mean	Std
Acceleration	Normal	42.3	0.22
Deceleration	Normal	16.57	0.065
Port Stay	Normal	14.13	0.001
Cruising	Normal	509.1	4.5

Fitting results between fitted distribution and simulation results are presented in the graph below:

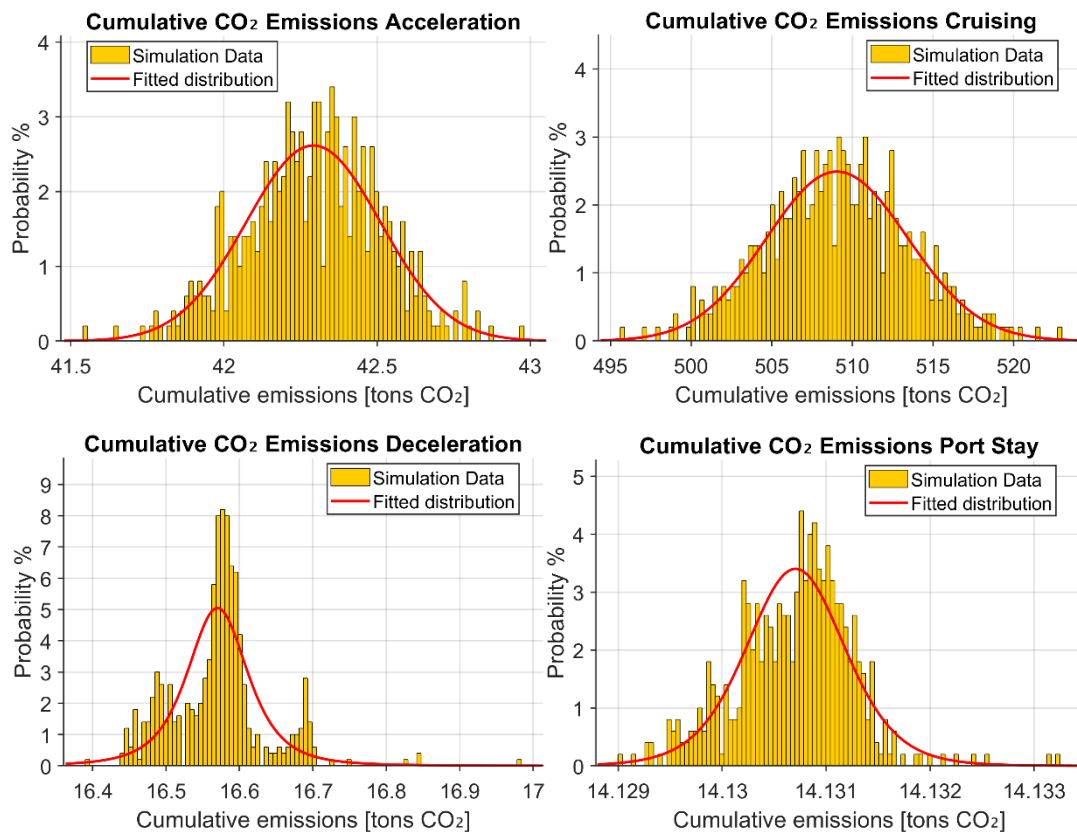


Figure 30 Fitted distributions for each trip phase (Use case 2).

To quantify the variability in cumulative CO₂ emissions, we extracted key distribution quantiles from the best-fitting probabilistic model. The 5th percentile represents a conservative best-case scenario, the 50th percentile corresponds to the typical (median) expected performance, and the 95th percentile reflects a worse-case upper bound under normal operating uncertainty. These quantile values provide a direct, model-based characterization of the system's expected, optimistic, and pessimistic outcomes, enabling clear comparison of reliability and



risk. Table 17 summarizes the estimated emission levels at each quantile and also the minimum and maximum observed values.

Table 17 Percentile Distribution of Vessel Trip Phase Emissions (use case 2).

Trip Phase	5th	50th	95th
Acceleration	41.93	42.29	42.65
Deceleration	16.47	16.57	16.67
Port Stay	14.13	14.131	14.132
Cruising	501.9	509.1	516.35

Based on the percentiles the following are true:

5th percentile

- Only 5% of all possible outcomes are expected to be below this value.
- This is effectively a best-case optimistic scenario.

50th percentile

- This is the median, meaning half of the outcomes are below and half above.
- This represents the typical or central behavior of the system.

95th percentile

- 95% of all outcomes are below this value.
- Only 5% of runs exceed this level.
- This represents a worst case but still realistic scenario.

4.1.3 Hypotheses Analysis on input variables

The results of the one sample K-S test are represented here. The K-S test was used to examine if the drawn sample for each input parameter is representative of the population. If the sampled distributions were not consistent with their populations, the simulation could produce biased/incorrect results. The *p* – values for all the input parameters are presented in the following table:

Table 18 K-S test results (use case 2)

Parameter	K-S result (p-value)	Interpretation
Capacitor Capacitance	1	Sample is consistent
Wind Speed	1	Sample is consistent
Wind Direction	1	Sample is consistent
Current Velocity	1	Sample is consistent
Wave Height	1	Sample is consistent
Wave period	1	Sample is consistent
Wave direction	1	Sample is consistent
Ambient Temperature	1	Sample is consistent
Ambient Pressure	1	Sample is consistent
Ship mass loading	1	Sample is consistent

Since the p-value for all parameters is 1, we fail to reject the H0 hypothesis and we can safely conclude that all samples are representative of their respective population distribution. This makes the results of the MC consistent.

4.2 Sensitivity Analysis on Input Variables

Spearman correlation provides normalized values ($\rho_s \in [-1, +1]$) that are directly interpretable: variables with $|\rho_s| > 0.7$ indicate strong influence to total emissions, while the sign reveals whether increasing the input increases or decreases emissions.

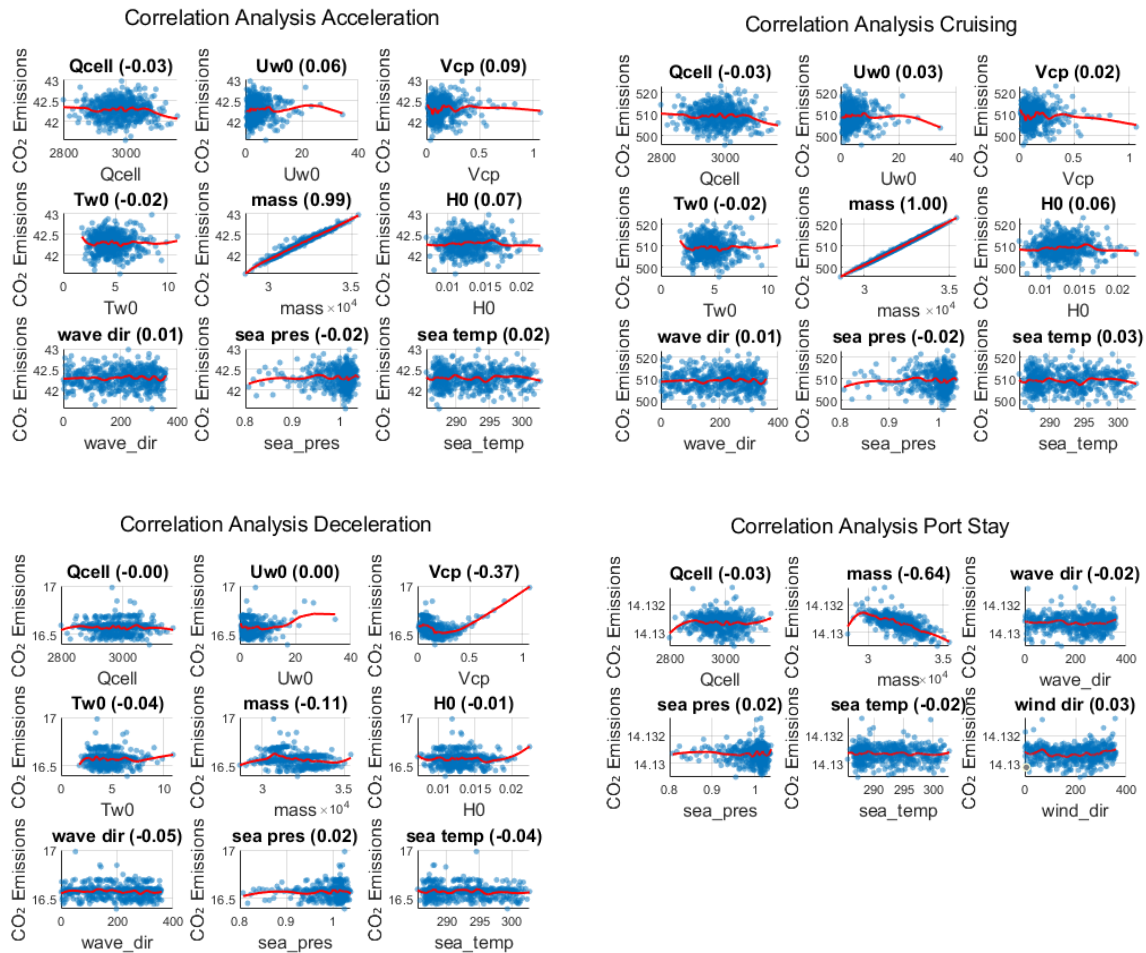


Figure 31 Spearman correlation coefficients for input variables

When all the variables are varied simultaneously, the ones that have a direct influence on the total CO2 emissions are the current speed, wave height and the capacity of the battery which affects the available energy during the port stay. Again, to quantify the magnitude of impact on the CO2 emissions we use the multilinear regression method.

4.3 Reduced surrogate models

The multilinear regression model was fitted to explain and predict cumulative CO₂ emissions using the most informative input variables for every trip phase, meaning we used the top ranked variables based on the Mutual Information towards the target variable.

A summary of the selected predictors, their standardized coefficients, is provided in Figure 32.

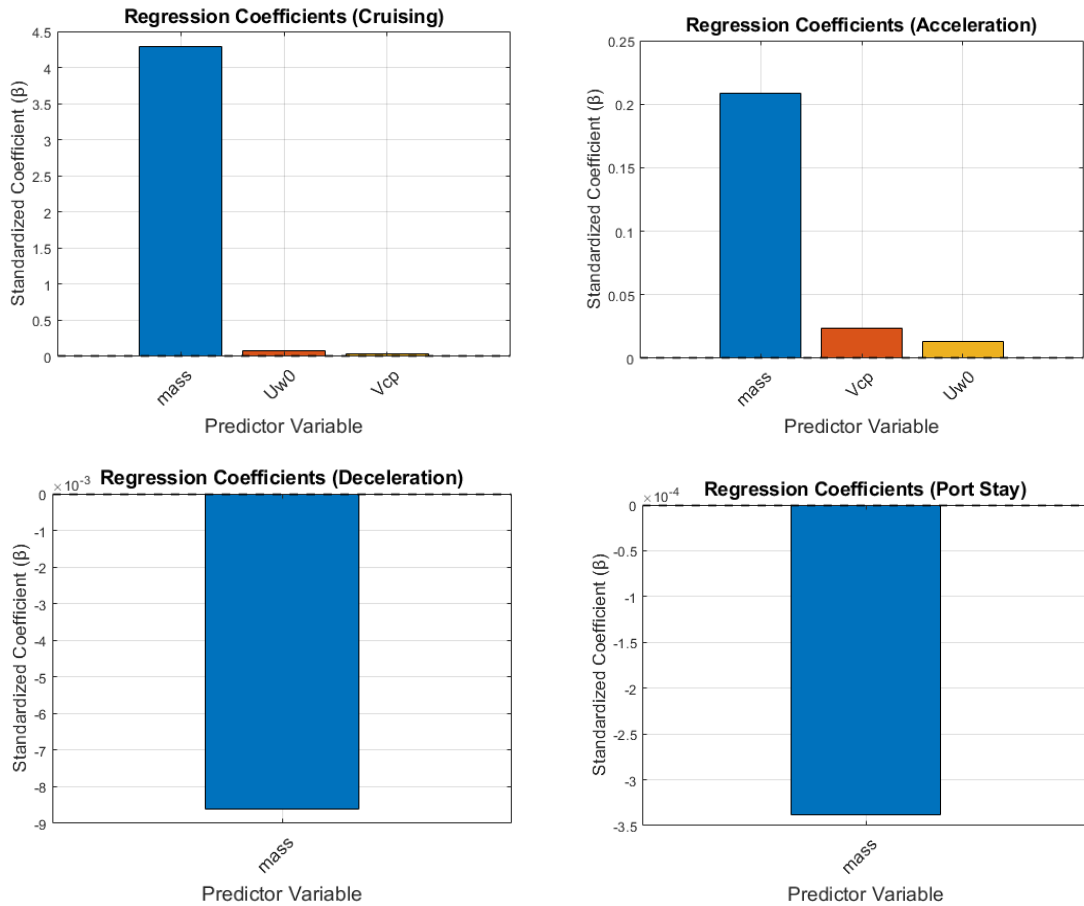
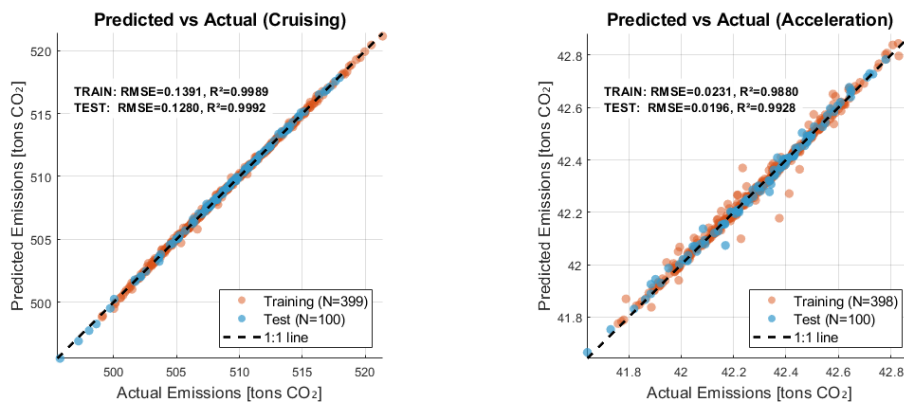


Figure 32 Multilinear regression analysis standardized coefficients.

Results for port stay emissions can be ignored as will be explained below. This can be seen by the very low regression coefficients that are calculated for these phases. Fitted Model performance is presented in Figure 33.



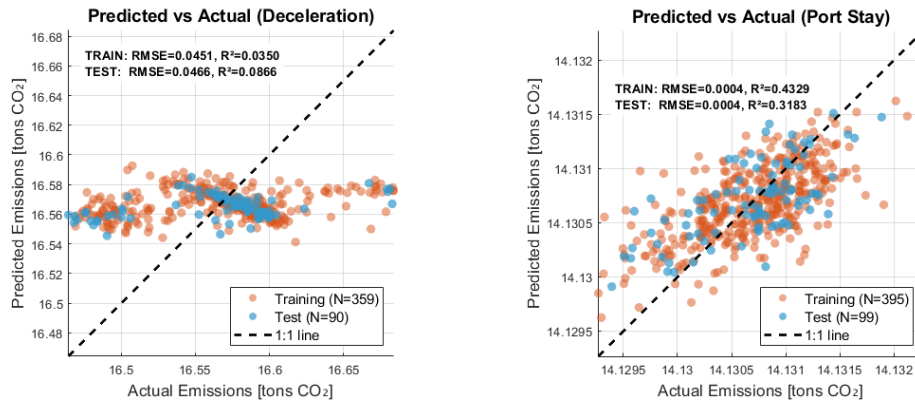


Figure 33 Predicted vs Actual Values for CO₂ emissions. Performance characterization of the multilinear regression analysis (Use case 2).

Prediction performance is good for both cruising and acceleration phase with low RMSE and high R² values.

The prediction performance for deceleration is poor (RMSE = 0.466, R² = 0.0860), with significant scatter around the 1:1 line. The model struggles to capture the variability in deceleration emissions, indicating that additional features or nonlinear relationships may be needed to accurately predict this phase.

Port stay emissions are highly clustered around a single value (~14.13 tons CO₂), exhibiting near-deterministic behavior (RMSE = 0.004, R² = 0.3183). Since the emissions show minimal variability, any prediction is unnecessary and port stay can be treated as a constant value.

5 Results for use case 3

5.1 Cumulative CO₂ Emissions Results

5.1.1 Cumulative Emissions distribution comparison

The Anaconda vessel operates mainly in inland waterways rather than at sea. Because of this, our analysis does not segment the operational profile into the typical phases seen in seagoing vessels, such as navigation, port time, and maneuvering. Instead, we run the Monte Carlo simulation to account for total CO₂ emissions over the entire trip, without splitting it into distinct phases.

The overall trip results are provided in the table below where the absolute values in terms of CO₂ are depicted for the entire trips as well as per trip mode along with the percentage difference achieved after AENEAS.

Table 19 Comparison of cumulative CO₂ emissions over the full duration for a single run (use case 3).

	Total
Baseline (tn CO ₂)	39.34
Optimized (tn CO ₂)	38.73
Difference %	-1.56

Whole trip Comparison between Base and Optimized electrified architecture

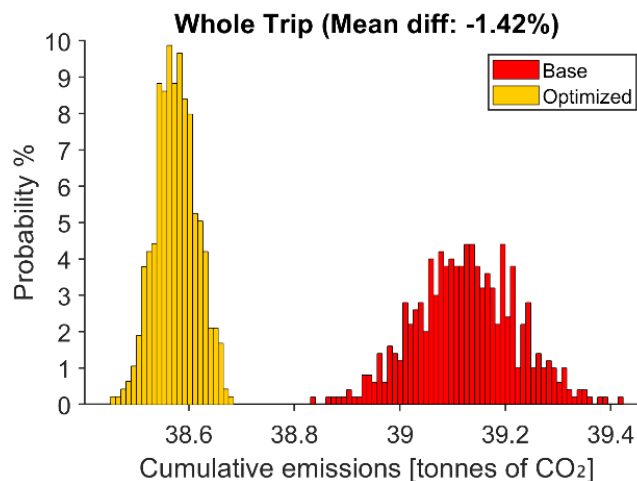


Figure 34 Probability distribution comparison for the whole trip between base and optimized vessel architecture (Case 3).

Again based on the results of the MC simulation for the whole trip Figure 34, we can clearly see a reduction of both the mean value and the CV for the total CO₂ emissions, meaning that the results now are less stochastic and more robust.

Table 20 Aggregated results for the mean value difference of CO₂ emissions for the specific MC trip (use case 3).

	Total
Baseline (tn CO ₂)	39.12
Optimized (tn CO ₂)	38.58

Difference %	-1.42
--------------	-------

5.1.2 Target variable distribution identification and characterization

The distribution characteristics of the target variable for every trip phase for the optimized architecture is presented in the following table:

Table 21 Results for the best fitted distribution for each trip phase (use case 3).

Trip Phase	Distribution Type	Mean	Std
Whole trip	Normal	38.58	0.04

Fitting results between fitted distribution and simulation results are presented in the graph below:

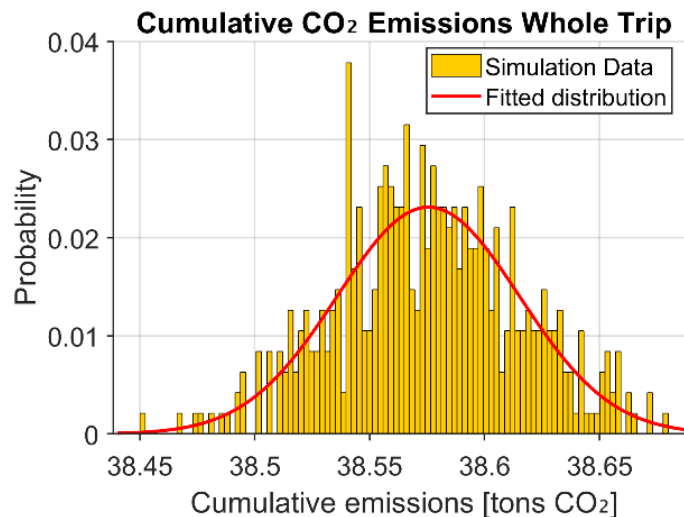


Figure 35 Fitted distribution for Cumulative CO2 emissions (Case 3).

Again, to quantify the variability in cumulative CO₂ emissions, we extracted key distribution quantiles from the best-fitting probabilistic model.

Table 22 Percentile Distribution of Vessel Trip Phase Emissions (use case 3).

Trip Phase	5th	50th	95th
Acceleration	38.51	38.58	38.65

Based on the percentiles the following are true:

5th percentile

- Only 5% of all possible outcomes are expected to be below this value.
- This is effectively a best-case optimistic scenario.

50th percentile

- This is the median, meaning half of the outcomes are below and half above.
- This represents the typical or central behavior of the system.

95th percentile

- 95% of all outcomes are below this value.
- Only 5% of runs exceed this level.
- This represents a worst case but still realistic scenario.

5.1.3 Hypotheses Analysis on input variables

The results of the one sample K-S test are represented here.

Table 23 K-S test results (use case 3).

Parameter	K-S result (p-value)	Interpretation
Cell Capacity	1	Sample is consistent
Wind Speed	1	Sample is consistent
Wind Direction	1	Sample is consistent
Current Velocity	1	Sample is consistent
Ambient Temperature	1	Sample is consistent
Ambient Pressure	1	Sample is consistent
Ship mass loading	1	Sample is consistent

Since the p-value for all parameters is 1 we fail to reject the H0 hypothesis and we can safely conclude that all samples are representative of their respective population distribution.

5.2 Sensitivity Analysis on Input Variables

Spearman correlation provides normalized values ($\rho_s \in [-1, +1]$) that are directly interpretable: variables with $|\rho_s| > 0.7$ indicate strong influence to total emissions, while the sign reveals whether increasing the input increases or decreases emissions.

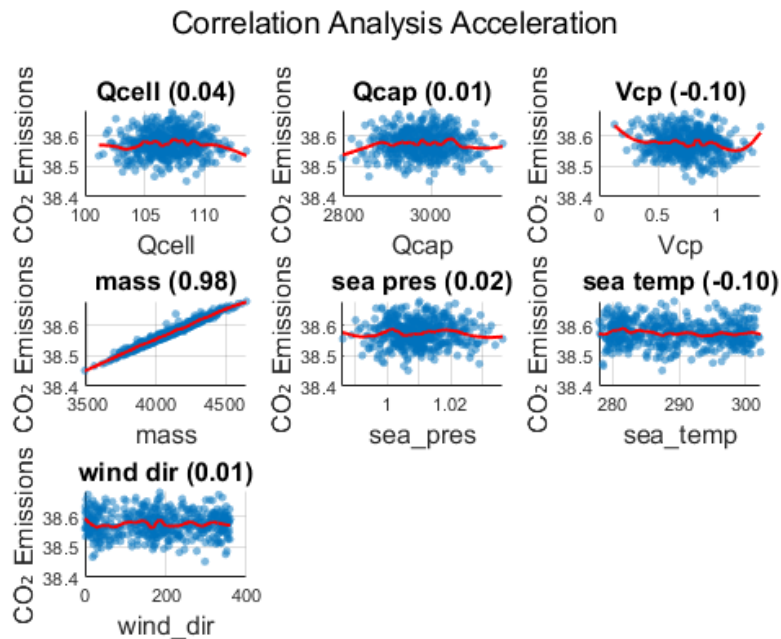


Figure 36 Spearman correlation coefficients for input variables (Case 3).

5.3 Reduced surrogate models

A summary of the selected predictors, their standardized coefficients, is provided in Figure 27.

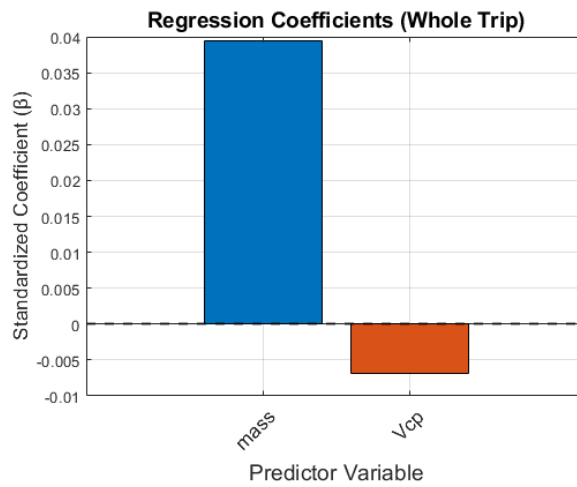


Figure 37 Multilinear regression analysis standardized coefficients (Case 3).

Two variables are enough to predict with high relative accuracy the CO2 emissions on this case. Fitted Model performance is presented in Figure 28:

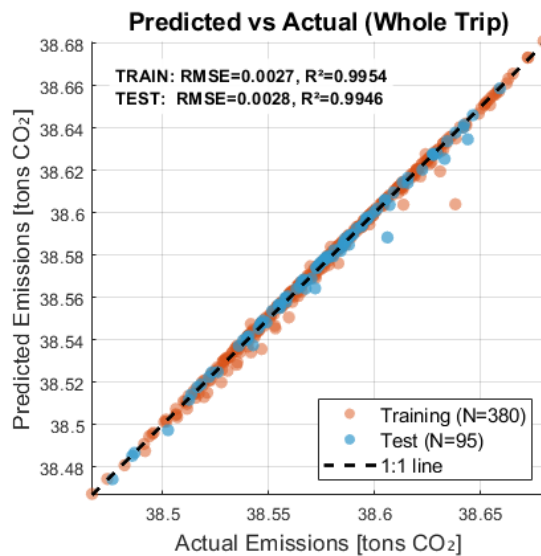


Figure 38 Predicted vs Actual Values for CO2 emissions. Performance characterization of the multilinear regression analysis (Case 3).

6 Conclusions

This deliverable validated the optimized AENEAS electrified energy storage architectures using a Monte Carlo–based digital twin framework, ensuring that all reported performance gains account for realistic uncertainty in operational conditions, environmental inputs, and system parameters. The probabilistic assessment provides statistically robust evidence of CO₂ emission reductions and system robustness across three representative maritime use cases.

For use-case 1 (short-sea Ro-Ro vessel), Monte Carlo simulations demonstrate that the optimized architecture achieves a mean reduction of total cumulative CO₂ emissions of approximately -1% over the full trip. Phase-resolved MC results show that emission reductions are concentrated in near-shore operating modes, with mean reductions of -19.6% during acceleration, -13.0 % during deceleration, and -5.7 % during port stays. In contrast, cruising emissions exhibit a small mean increase of +0.7 %, attributed to higher battery charging rates and associated conversion losses. Importantly, the probability distributions for baseline and optimized configurations retain similar shapes and spreads, indicating that the optimized architecture preserves robustness and does not amplify uncertainty-driven emission extremes.

For use-case 2 (short-sea Ro-Pax vessel), Monte Carlo results confirm the effectiveness of the hybrid battery–supercapacitor architecture in reducing emissions during maneuvering and port operations. The optimized configuration achieves a mean total CO₂ emission reduction of -1.63 % over the full Monte Carlo trip. Phase-level analysis shows no measurable change during cruising (0 %), while acceleration emissions are reduced by approximately -2.7 %, deceleration emissions by -31.5 %, and port-stay emissions by -22.25 %. The deceleration phase additionally exhibits a reduction in variance, indicating improved predictability and robustness under uncertainty. These results demonstrate that supercapacitors are particularly effective for mitigating transient power demands close to shore, without compromising system-level stability.

For use-case 3 (inland shipping vessel), where the operational profile is assessed at whole-trip level rather than phase-resolved, Monte Carlo simulations indicate a mean reduction in total cumulative CO₂ emissions of -1.42 % for the optimized architecture of hybridization. The optimized system achieves a reduction of the mean cumulative emissions, while also reducing the coefficient of variation, resulting in a narrower and more predictable emission distribution, confirming increased robustness under operational uncertainty. These results demonstrate that the AENEAS electrification concepts are applicable and effective in inland waterway contexts, despite fundamentally different operating characteristics compared to seagoing vessels.

Across all three use cases, the Monte Carlo analysis consistently shows that the optimized AENEAS architectures deliver statistically significant emission reductions, particularly in environmentally sensitive operating phases such as maneuvering and port stay, while maintaining or improving robustness under uncertainty. The preservation of distribution shape and variance, combined with systematic shifts toward lower mean emissions, confirms that the observed benefits are not scenario-dependent but structurally embedded in the optimized system designs. These findings provide a strong quantitative foundation for further scaling, integration, and demonstration of the AENEAS energy storage solutions in future research projects and actual application practice.

7 References

- [1] “Simcenter Amesim, Version 2310, Build 2023-10-20, Siemens Digital Industries Software. Platform: Windows 10/11.”
- [2] “Holtrop-Approximate-1982”.
- [3] “Ventura, M. Estimation Methods for Basic Ship Design. Ship Design . Instituto Superior Técnico.”
- [4] “Parson, M. Parametric Design. Ship Design and Construction. Chapter 11. Vol I. 2003.”
- [5] “Copernicus Climate Change Service (C3S), ‘ERA5 hourly data on single levels from 1940 to present,’ Climate Data Store (CDS), Data set, Jun. 14, 2018. doi: 10.24381/cds.adbb2d47. Accessed: Jan. 8, 2026.”
- [6] “Copernicus Marine Service, ‘Copernicus Marine MyOcean Expert Viewer,’ Copernicus Marine Data Store, Web application. Accessed: Jan. 8, 2026. [Online]. Available: <https://data.marine.copernicus.eu/viewer/expert?view=viewer&basemap=dark&crs=epsg:4326&layers=...>”
- [7] F. Hakimi, “Robust estimation with latin hypercube sampling: a central limit theorem for Z-estimators,” Feb. 2025, [Online]. Available: <http://arxiv.org/abs/2502.06321>
- [8] W. Tong, W. Q. Koh, E. Birgersson, A. S. Mujumdar, and C. Yap, “Correlating uncertainties of a lithium-ion battery - A Monte Carlo simulation,” *Int J Energy Res*, vol. 39, no. 6, pp. 778–788, May 2015, doi: 10.1002/er.3282.

8 Acknowledgements and disclaimer

The author(s) would like to thank the partners in the project for their valuable comments on previous drafts and for performing the review

#	Partner	Partner full name
1	FM	FLANDERS MAKE
2	CEA	COMMISSARIAT A L ENERGIE ATOMIQUE ET AUX ENERGIES ALTERNATIVES
3	ABEE	AVESTA BATTERY & ENERGY ENGINEERING
4	SIE	SIEMENS INDUSTRY SOFTWARE SAS
5	UVA	VAASAN YLIOPISTO
6	I2M	I2M UNTERNEHMENSENTWICKLUNG GMBH
7	GRIM	GRIMALDI EUROMED SPA
8	INLS	INLAND SHIPPING SRL
9	FV	FUNDACION DE LA COMUNIDAD VALENCIANA PARA LA INVESTIGACION, PROMOCION Y ESTUDIOS COMERCIALES DE VALENCIAPORT
10	SOER	FUNDACION CENTRO TECNOLOGICO SOERMAR
11	FMAR	FORMARE- POLO NAZIONALE PER LO SHIPPING SRL
12	ISSN	INSTITUTE FOR SUSTAINABLE SOCIETY AND INNOVATION
13	FS	CONSTRUCCIONES NAVALES P FREIRE SA

LEGAL DISCLAIMER

Copyright ©, all rights reserved. No part of this report may be used, reproduced and or/disclosed, in any form or by any means without the prior written permission of AENEAS and the AENEAS Consortium. Persons wishing to use the contents of this study (in whole or in part) for purposes other than their personal use are invited to submit a written request to the project coordinator.

The authors of this document have taken any available measure in order for its content to be accurate, consistent and lawful. However, neither the project consortium as a whole nor the individual partners that implicitly or explicitly participated in the creation and publication of this document shall be liable or responsible, in negligence or otherwise, for any loss, damage or expense whatever sustained by any person as a result of the use, in any manner or form, of any knowledge, information or data contained in this document, or due to any inaccuracy, omission or error therein contained.



Funded by
the European Union

9 Abbreviations and Definitions

Term	Definition
AE	Auxiliary Engine
DG	Diesel Generator
ICE	Internal Combustion Engine
ME	Main Engine
BOL	Beginning of Life
MC	Monte Carlo
SSSB	Semi-solid-state battery
SC	Super capacitors
ESS	Energy storage systems
EMS	Energy Management Strategy
PMS	Power Management Strategy
EOL	End of life
SOC	State of Charge
PDF	probability density function
KDE	Kernel density estimation
MI	Mutual Information
K-S	Kolmogorov–Smirnov Test
H&M	Holtrop and Mennen resistance prediction method
RC	Resistance-Capacitance
RO-RO	Roll-On / Roll-Off vessel
RO-PAX	Roll-On / Roll-Off Passenger vessel
WP	Work Package
TRL	Technology Readiness Level

List of Figures

Figure 1 Example route of the Grimaldi RO-RO vessel used in the Amesim simulation.....	15
Figure 2 Hybrid Ro-Ro ship powertrain topology as modeled in Simcenter Amesim.....	16
Figure 3 MEs (left) and AEs (left) average operating load for the hybrid (red) and a non-hybrid similar ship (blue).....	17
Figure 4 Model validation comparing actual recordings with model estimations for ME power (left) and battery SOC (right).	19
Figure 5 Figure showcasing the optimized battery charging strategy: avoiding charge during port or maneuvering phase.....	20
Figure 6 Example route of the Grimaldi RO-PAX vessel used in the Amesim simulation.....	21
Figure 7 Hybrid Ro-Pax ship powertrain topology as modeled in Simcenter Amesim.....	22
Figure 8 MEs (left) and AEs (right) average operating load for the hybrid (red) and a non-hybrid similar ship (blue).....	23
Figure 9 Comparison of main engine power between model and recordings.	24
Figure 10 Peak Shaving strategy for DG1 using the Supercapacitors during the maneuvering (acceleration and deceleration between one port stay).....	26
Figure 11 Supercapacitor and battery pack power split during operation.	26
Figure 12 SOC of base model vs SOC of the optimized vessel with the SC and the new EMS.	27
Figure 13. Example route of the Inland shipping ANACONDA vessel route and speed profile	28
Figure 14 Comparison of main engine loading point, model vs recordings.	29
Figure 15 Model in Simcenter Amesim with the updated layout of hybridization	30
Figure 16 Power split comparison Base vs Optimized architecture for use case 3.....	31
Figure 17 Use case 1 variables distribution.	32
Figure 18 Use case 2 variables distributions.	33
Figure 19 Use case 3 variables distributions.	33
Figure 20 Schematic of Monte Carlo Methodology	34
Figure 21 MATLAB-Amesim scripted based communication	35
Figure 22 Latin Hypercube coverage of the parametric space vs random sampling for 50 total samples for a random variable.	36
Figure 23 Probability distribution comparison for different trip phases between base and optimized vessel architecture (Use case 1).	41
Figure 24 Fitted distributions for each trip phase (Use case 1).	43
Figure 25 K-S results for wave height and wave period (Use case 1).	45
Figure 26 Spearman correlation coefficients for input variables (Use case 1).	46
Figure 27 Multilinear regression analysis standardized coefficients (Use case 1).	47
Figure 28 Predicted vs Actual Values for CO2 emissions. Performance characterization of the multilinear regression analysis (Use case 1).	47
Figure 29 Probability distribution comparison for different trip phases between base and optimized vessel architecture (Use case 2).	50
Figure 30 Fitted distributions for each trip phase (Use case 2).	51
Figure 31 Spearman correlation coefficients for input variables	53
Figure 32 Multilinear regression analysis standardized coefficients.	54
Figure 33 Predicted vs Actual Values for CO2 emissions. Performance characterization of the multilinear regression analysis (Use case 2).	55
Figure 34 Probability distribution comparison for the whole trip between base and optimized vessel architecture (Case 3).	56
Figure 35 Fitted distribution for Cumulative CO2 emissions (Case 3).	57

Figure 36 Spearman correlation coefficients for input variables (Case 3).58
Figure 37 Multilinear regression analysis standardized coefficients (Case 3).59
Figure 38 Predicted vs Actual Values for CO2 emissions. Performance characterization of
the multilinear regression analysis (Case 3).59



List of tables

Table 1 Key parameters of the Holtrop & Mennen ship resistance prediction method.....	11
Table 2 Ro-Ro ship geometric characteristics necessary for the Holtrop and Mennen method (use case 1).	18
Table 3 New vs old Ro-Ro ship topology modifications (use case 1).	19
Table 4 Ro-Pax ship geometric characteristics necessary for the Holtrop and Mennen method (use case 2).	24
Table 5 New vs old Ro-Pax ship topology modifications (use case 2).	25
Table 6 Geometric characteristics necessary for the Holtrop and Mennen method (use case 3).	28
Table 7 New vs old ship topology modifications (use case 3).	29
Table 8 Parameters used to perform the MC simulation of the optimized architectures	32
Table 9 Comparison of cumulative CO ₂ emissions over the full duration for a single run (use case 1).	40
Table 10 Aggregated results for the mean value difference of CO ₂ emissions for the specific MC trip (use case 1).	41
Table 11 Results for the best fitted distribution for each trip phase for the optimized architecture (use case1).	42
Table 12 Percentile Distribution of Vessel Trip Phase Emissions (use case 1).	44
Table 13 K-S test results (use case 1).	44
Table 14 Comparison of cumulative CO ₂ emissions over the full duration for a single run (use case 2).	49
Table 15 Aggregated results for the mean value difference of CO ₂ emissions for the specific MC trip (use case 2).	50
Table 16 Results for the best fit distribution for each trip phase for the optimized architecture (use case 2).	51
Table 17 Percentile Distribution of Vessel Trip Phase Emissions (use case 2).	52
Table 18 K-S test results (use case 2).	52
Table 19 Comparison of cumulative CO ₂ emissions over the full duration for a single run (use case 3).	56
Table 20 Aggregated results for the mean value difference of CO ₂ emissions for the specific MC trip (use case 3).	56
Table 21 Results for the best fitted distribution for each trip phase (use case 3).....	57
Table 22 Percentile Distribution of Vessel Trip Phase Emissions (use case 3).	57
Table 23 K-S test results (use case 3).	58